THE ADSORPTIVE REMOVAL OF ANTIBIOTIC CIPROFLOXACIN FROM AQUEOUS MEDIUM BY USING BANANA PEEL

By

RENEE CLAIRE VOON ZI-YIN

A project report submitted to the Department of Chemical Science

Faculty of Science

Universiti Tunku Abdul Rahman

in partial fulfilment of the requirements for the degree of

Bachelor of Science (Hons) Chemistry

Jan 2025

COPYRIGHT STATEMENT

ABSTRACT

THE ADSORPTIVE REMOVAL OF ANTIBIOTIC CIPROFLOXACIN FROM AQUEOUS MEDIUM BY USING BANANA PEEL

RENEE CLAIRE VOON ZI-YIN

This research explores the adsorption of ciprofloxacin (CIP) from aqueous solutions using banana peel (BP) as an adsorbent. The goals include figuring out the removal efficiency under various conditions, characterizing BP and figuring out the isotherms and adsorption kinetics. According to the study, CIP's adsorption onto BP rose with increasing agitation rate, adsorbent dosage, and contact time. The adsorption process adhered to the Freundlich isotherm and followed the Pseudo-Second Order kinetic model, showing optimal effectiveness at pH levels above 4. The maximum CIP adsorption capacity by BP was 37.037 mg/g. SEM and AFM analyses verified surface changes in BP before and after adsorption, while the FTIR study suggested functional group involvement in the CIP-BP interaction. The significant factors that mainly contributes to the adsorption process was determined by Plackett-Burman Design, and the optimized condition equation was determined by Response Surface Methodology. BP shows great potential as an eco-friendly and cost-effective adsorbent for the removal of CIP from water, and additional modifications could further enhance both its adsorption capacity and practical utility.

ABSTRAK

PENYINGKIRAN ADSORPTIF ANTIBIOTIK CIPROFLOXACIN DARI LARUTAN AKUOUS MENGGUNAKAN KULIT PISANG

RENEE CLAIRE VOON ZI-YIN

Kajian ini menunjukkan penjerapan ciprofloxacin (CIP) oleh kulit pisang (BP) daripada larutan akueus. Objektif kajian ini termasuk menentukan kecekapan penyingkiran di bawah pelbagai keadaan, mencirikan BP, serta menentukan model isoterm dan kinetik penjerapan. Menurut kajian ini, penjerapan CIP ke atas BP meningkat dengan peningkatan kadar pengacauan, dos bahan penjerap, dan masa sentuhan. Penjerapan tersebut mengikut model isoterm Freundlich dan model kinetik Pseudo-Order Kedua, dan ia paling berkesan pada nilai pH melebihi 4. Kapasiti penjerapan maksimum CIP oleh BP ialah 37.037 mg/g. Analisis SEM dan AFM mengesahkan perubahan dalam morfologi permukaan dan topografi BP sebelum dan selepas penjerapan, manakala kajian FTIR mencadangkan penglibatan kumpulan berfungsi dalam interaksi antara CIP dan BP. Faktor-faktor penting yang paling banyak menyumbang kepada proses penjerapan telah dikenal pasti menggunakan Reka Bentuk Plackett-Burman, manakala persamaan keadaan optimum telah ditentukan menggunakan Kaedah Permukaan Tindak Balas (RSM). BP merupakan bahan penjerap yang berpotensi, mesra alam dan kos efektif untuk penyingkiran CIP daripada air, dan pengubahsuaian lanjut boleh meningkatkan prestasi dan keberkesanan praktikalnya.

Keywords: Adsorption; Antibiotics; Banana Peel; Kinetics; Isotherm

Subject Area: QD1-65 General

ACKNOWLEDGEMENT

I would like to convey my deepest appreciation to all individuals who have offered their support throughout my Final Year Project at UTAR.

I would like to extend my profound appreciation to my supervisor, Dr. Ong Siew Teng, for her unwavering guidance, support, and encouragement throughout the course of this research. Her expertise, critical insights, and steadfast motivation were vital to the successful completion of this work.

I am grateful towards my besties for their constant encouragement, understanding, and the many discussions that helped me maintain focus and motivation throughout this journey. Their encouragement and companionship made the challenging moments more bearable and the journey more enjoyable.

I am deeply indebted to my family for their unconditional love, enduring patience, and unfailing encouragement. Their unwavering belief in my abilities served as a source of motivation, enabling me to maintain the strength and determination needed to see this project through to completion. Without their sacrifices and encouragement, this achievement would not have been possible.

Thank you.

TABLE OF CONTENTS

LIST OF TABLES

LIST OF FIGURES

LIST OF SYMBOLS / ABBREVIATIONS

C_e	Concentration of CIP at equilibrium, mg/L
C_0	Initial CIP concentration, mg/L
C_S	CIP concentration at saturation, mg/L
C_t	CIP concentration at time, mg/L
h	Initial adsorption rate, mg/g min
K_B	BET constant
K_L	Langmuir isotherm, L/mg
K_F	Freundlich isotherm constant, mg/g
k_1	Pseudo-first order kinetics rate constant, min^{-1}
k_2	Pseudo-second order kinetics rate constant, g/mg min
m	Mass of Banana Peel, g
n	Freundlich constant for intensity
q_e	Amount of CIP adsorbed at equilibrium, mg/g
$q_{e, cal}$	Calculated q_e value
$q_{e, exp}$	Experimental q_e value
q_m	Maximum adsorption capacity of BP, mg/g
q_t	Amount of CIP adsorbed at time t, mg/g
R_L	Equilibrium parameter
t	Time, min
V	Volume of dye solution, L

AC	Activated Carbon
AC-CoR I	H_3PO_4 - activated coffee residue carbon
AC-CoR II	H_3PO_4 & $FeCl_3$ - activated coffee residue carbon
AC-CoR III	$FeCl_3$ - activated coffee residue carbon
AFM	Atomic Force Microscopy
As	Arsenic
AWS	Wheat Straw
BET	Brunauer-Emmett-Teller
BP	Banana Peel
BPAC	Banana peel-based activated carbon
BPBC	Banana Peel Biochar
Cd	Cadmium
CIP	Ciprofloxacin
Cr	Chromium
CS	Chitosan
CS-MNPs	Chitosan-magnetite composites
FTIR	Fourier Transform-Infrared Spectroscopy
HCl	Hydrochloric Acid
Hg	Mercury
KBr	Potassium Bromide
MB	Methylene Blue
MG	Malachite Green
MNPs	Magnetite
NaOH	Sodium Hydroxide
PB	Plackett-Burman Design

Pb	Lead
PBC	Peanut Shell Biochar
PFO	Pseudo-first order
PSO	Pseudo-second order
PVP	Polyvinylpyrrolidone
R^2	Coefficient of Determination
RhAC	Rice husk activated carbon
rpm	Revolutions per minute
RSM	Response Surface Methodology
SCB	Sugarcane bagasse
SEM	Scanning Electron Microscopy
SMS	Surfactant-Modified Sepiolite
TC	Tetracycline
UV-Vis	Ultraviolet-Visible
WCR	Waste Coffee Residue
XRD	X-ray diffraction

CHAPTER 1

INTRODUCTION

1.1 Background

Antibiotic pollution in water systems is a developing environmental concern brought on by the use of antibiotics in agriculture, animal medicine, and human medicine. A significant amount of antibiotics that are eaten are eliminated in their active state and end up in wastewater systems through residential sewage, hospital effluents, and agricultural runoff. Another factor contributing to this problem is the direct discharge of poorly treated wastewater into natural water bodies by pharmaceutical manufacturing facilities.

Antibiotic residues have been finding their way into aquatic habitats more frequently since the mid-1900s, when industrial-scale antibiotic production started, especially with the large production of penicillin during World War II. The lack of early regulatory controls and the restricted capacity of traditional wastewater treatment plants (WWTPs), which are typically poor at eliminating antibiotic compounds, have made this contamination worse (Daughton & Ternes, 1999; WHO, 2012).

Since antibiotics were frequently used in animals to prevent disease and promote growth, the problem was exacerbated by the growth of intensive livestock production in the 1960s. Antibiotics can now infiltrate surface and groundwater through manure and farm runoff (Kümmerer, 2008).

In aquatic settings, antibiotics can damage ecosystems by upsetting microbial communities, decreasing biodiversity, and encouraging the emergence of diseases with resistance. Antibiotic-resistant bacteria (ARB) and antibiotic-resistant genes (ARGs) can be spread by drinking water, contaminated seafood, and recreational water use, and their persistence in water promotes their emergence and spread (Pabst, 2023).

The health of people is seriously threatened by antibiotic resistance. Treating resistant infections is difficult and require for second-line treatments that are less efficient and more costly. Increased mortality, longer hospital stays, and higher healthcare expenses result from this. One of the most urgent global health issues, according to the WHO, is antibiotic resistance (Kümmerer, 2009).

Adsorption is a well-known technique for eliminating antimicrobial pollutants from water because of its effectiveness, affordability, and ease of use. Antibiotic molecules build up on the surface of adsorbent materials during this process, which successfully lowers the concentration of antibiotics in aqueous solutions. Common adsorbents like activated carbon, biochar and biomass-based adsorbents and natural clays are effective in removing antibiotic waste from water. (Eniola, Kumar & Barakat, 2019)

Despite the effectiveness of adsorption, issues including adsorbent regeneration and reuse, wasted material disposal, and the possibility of antibiotic desorption back into the environment must be addressed. To increase the sustainability of this process, research is still being done to create adsorbents with larger capacities, greater selectivity, and better regeneration qualities. (Das & Sengupta, 2023)

1.2 Problem Statements

Antibiotic residues in water pose a serious risk to public health and the environment (Akhter et.al., 2024). Antibiotic residues in drinking water sources raise the possibility of human exposure. Despite the generally modest quantities, long-term exposure can lead to toxicity, allergic responses, and the emergence of diseases that are resistant to antibiotics (Karonlinska, 2023). Studies show that over 100,000 tons of antibiotics enter the environment each year, and aquatic environments are especially at risk from sewage runoff from homes, hospitals, and farms (Mu et.al, 2023).

Numerous routes allow antibiotic waste to infiltrate aquatic habitats, raising serious issues for the environment and human health. Antibiotics that are unused or expired are disposed of in households, which pollutes the environment. Medications can evade sewage treatment systems and enter water bodies when people dispose of them incorrectly, such as by flushing them down the sink or toilet (Akhter et.al., 2024). Antibiotics are used in animal husbandry to prevent illnesses and encourage growth. Antibiotics can seep into soils and streams through the manure of treated animals, which is frequently used as fertilizer, particularly during periods of precipitation.

Antibiotics can linger in water and selectively affect microbial communities, which can lead to the emergence of bacteria that are resistant to them. Because these resistant strains can spread through water supplies, this directly endangers human health in addition to upsetting aquatic ecosystems (Karonlinska, 2023).

Removing antibiotic waste is challenging as numerous antibiotics are made to withstand deterioration, which enables them to endure in watery settings. Due

to their durability, water frequently contains trace levels of antibiotics, necessitating the use of extremely sensitive and effective removal techniques. Advanced treatment technologies are required to detect and eradicate such low quantities (Darvishi et.al., 2023). The creation and application of cutting-edge water treatment technologies are necessary to meet these difficulties, therefore, adsorption is one efficient method for eliminating antibiotic waste from water.

1.3 Antibiotics

Antibiotics are mostly used to treat animal and human bacterial diseases. The chemical structure of antibiotics, which frequently corresponds with their spectrum of activity and mechanism of action, can be used to categorize them. Their pharmacological characteristics and possible clinical uses are better understood thanks to this classification. Table 1.1 shows the classification of antibiotics based on their mechanism of actions and Table 1.2 shows the classification of antibiotics based on their spectrum of activity.

Table 1.1: Classification of antibiotics based on mechanism of action.

Mechanism of Action	**Antibiotic Classes**	**Examples**
Inhibition of Cell Wall Synthesis	β-lactams, Glycopeptides, Bacitracin	Penicillins (e.g., Amoxicillin), Cephalosporins (e.g., Ceftriaxone), Vancomycin
Inhibition of Protein Synthesis	Aminoglycosides, Tetracyclines, Macrolides, Lincosamides, Chloramphenicol, Oxazolidinones	Gentamicin, Doxycycline, Erythromycin, Clindamycin, Linezolid
Inhibition of Nucleic Acid Synthesis	Fluoroquinolones, Rifamycins	Ciprofloxacin, Rifampin
Inhibition of Folic Acid Synthesis	Sulfonamides, Trimethoprim	Sulfamethoxazole, Trimethoprim
Disruption of Cell Membrane Function	Polymyxins, Lipopeptides	Polymyxin B, Daptomycin

Source: Upmanyu & Malviya (2020)

Table 1.2: Classification of antibiotics based on spectrum of activity.

Spectrum of Activity	Description	Examples
Narrow-Spectrum	Effective against either Gram-positive or Gram-negative bacteria	Penicillin G, Vancomycin
Broad-Spectrum	Effective against a wide range of bacteria, including Gram-positive and Gram-negative types	Tetracyclines, Chloramphenicol

Source: Grada & Bunick (2021)

1.3.1 Ciprofloxacin (CIP)

Ciprofloxacin, a synthetic antibiotic, is renowned for its wide-ranging antibacterial activity and is part of the fluoroquinolone class. It was found in 1981 by researchers at Bayer Pharmaceuticals, who changed the structure of norfloxacin by substituting a cyclopropyl group for the ethyl group, greatly increasing the antibiotic's ability to combat Gram-negative bacteria. This change resulted in the creation of CIP, which was approved by the FDA for intravenous use in 1991 and for oral administration in 1987 (ACS, 2016).

The chemical formula of CIP is $C_{17}H_{18}FN_3O_3$, and its molecular weight is 331.4 g/mol. It is also known as 1-cyclopropyl-6-fluoro-1,4-dihydro-4-oxo-7-(1-piperazinyl)-3-quinolinecarboxylic acid. Its structure consists of a bicyclic

aromatic core with a piperazinyl group that improves its pharmacokinetic qualities and a fluorine atom that increases its antibacterial efficacy. Figure 1.1 shows the chemical structure of CIP. These structural changes make CIP effective against a variety of bacterial infections, contributing to its widespread prescription globally (Conley et al., 2018).

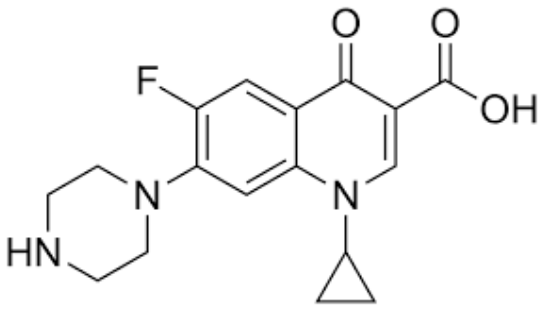

Figure 1.1: Chemical structure of ciprofloxacin

CIP has amine and carboxyl functional groups that cause it to behave amphoterically in aqueous media, resulting in pH-dependent speciation. At higher pH values, the molecule changes to an anionic form, but at lower pH values, it mostly exists in its cationic form. In aqueous environments, this pH-dependent speciation has a major impact on its interactions (Yu et al., 1994).

CIP's solubility in water is rather low and depends on several variables, including pH and the presence of other ions. Its bioavailability and efficacy in medicinal applications may be impacted by this restricted solubility.

1.3.2 Sources of CIP Wastes

There are several main ways that the commonly used fluoroquinolone antibiotic CIP enters aquatic habitats. Wastewater treatment plant (WWTP) effluent discharge is one important source. These factories frequently have trouble eliminating pharmaceutical substances entirely, which causes leftover antibiotics to leak into waterways. According to a study, CIP's hydrophilic properties let it move about in aquatic environments, which is why it was found in drinking water and WWTP effluents (Salah et al., 2024).

The agricultural industry, which uses CIP in animal husbandry, is another significant source. These methods can further contaminate aquatic habitats by releasing antibiotic residues into adjacent water sources (Akhter et al., 2024).

The careless disposal of unused or expired CIP in household waste significantly contributes to environmental pollution, especially in aquatic ecosystems. Medications are frequently introduced into wastewater systems through routine procedures like flushing them down the toilet or sink. The inability of wastewater treatment facilities to adequately remove all pharmaceutical substances, including antibiotics like CIP, results in their discharge into aquatic environments (OECD, 2022). The possible emergence of microorganisms resistant to antibiotics is one of the ecological hazards associated with CIP's presence in water bodies. Antibiotics' ability to effectively treat infections may be hampered by this resistance. CIP can also break down into hazardous metabolites that can damage aquatic life and disturb ecosystems (Salah et al., 2024).

1.4 Treatments

For the elimination of organic matter and nutrients, WWTP usually use secondary clarifying, biological treatments such activated sludge processes, and primary sedimentation. Nevertheless, pharmaceutical pollutants like CIP are frequently difficult to remove from wastewater using these conventional techniques. Since CIP is resistant to biodegradation due to its molecular stability and persistence, it has been found in surface waters, groundwater sources, and WWTP effluents (Al-Buriahi et al., 2022).

According to Arvia (2024), CIP may only be partially broken down by traditional treatment methods, leaving it unremoved and perhaps forming transformation products that could still be hazardous to the environment.

1.5 Adsorbents

Several adsorbents, including activated carbon, biochar, layered double hydroxides, hydrogels, and chitosan-based adsorbents, have been examined for the removal of CIP from wastewater. The bar chart in Figure 1.2 illustrates the adsorption capacities of different types of adsorbent materials based on various number of research. It shows that C@silica core/shell nanoparticles from zeolitic imidazolate framework-8 (ZIF-8) have the highest adsorption capacity of CIP removal from aqueous medium following by using ordered carbon as adsorbent.

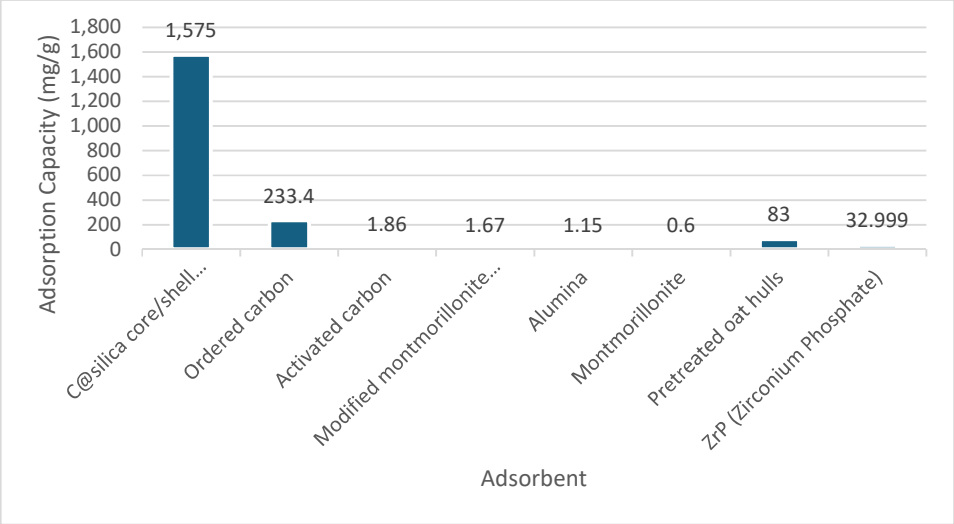

Figure 1.2: Adsorbent used for treating antibiotic-contaminated wastewater.

CIP is adsorbed from aqueous solutions via a variety of processes, most of which are impacted by the physicochemical characteristics of the antibiotic molecule and the adsorbent. The ionization of CIP and the surface charge of the adsorbent are key factors affecting adsorption. The cationic CIP and the negatively charged adsorbent surfaces experience electrostatic attraction at specific pH values, which improves adsorption efficiency. Moreover, the adsorption process can be aided by hydrogen bonding between functional groups like hydroxyl, carboxyl, and amino groups on the adsorbent and CIP (Su et al., 2024).

The adsorption capacity of adsorbents is further enhanced when they possess high specific surface areas and well-developed porous structures, as these features provide additional active sites for CIP molecules. Bamboo biochar, for instance, demonstrates efficient CIP adsorption due to its large surface area and porous design (Pham et al., 2023). Well-developed porous materials allow CIP molecules to diffuse and be accommodated inside their matrix (Käärik et al., 2024). According to studies on nitrogen-doped mesoporous carbon materials,

adsorption capacity is greatly influenced by the distribution of pore sizes, with some pore sizes being more suited for CIP adsorption (Lu et al., 2020).

1.5.1 Banana Peel (BP)

BPs, which are frequently regarded as agricultural waste, have drawn interest as an affordable and environmentally beneficial adsorbent for eliminating pollutants like CIP from wastewater. They are appropriate for adsorption processes due to their rich functional group composition, biodegradability, and inherent abundance. Furthermore, BPs are considered as cheap and sustainable substitute for traditional adsorbents due to their abundance and biodegradability. The banana, particularly the Cavendish variety, is among the most extensively cultivated and consumed fruits globally, representing approximately 47% of worldwide production, or 50 million tonnes annually. Because of this massive production, BPs are produced in large quantities. Their application supports sustainable wastewater treatment methods in addition to addressing waste management issues (Gupta et al., 2025).

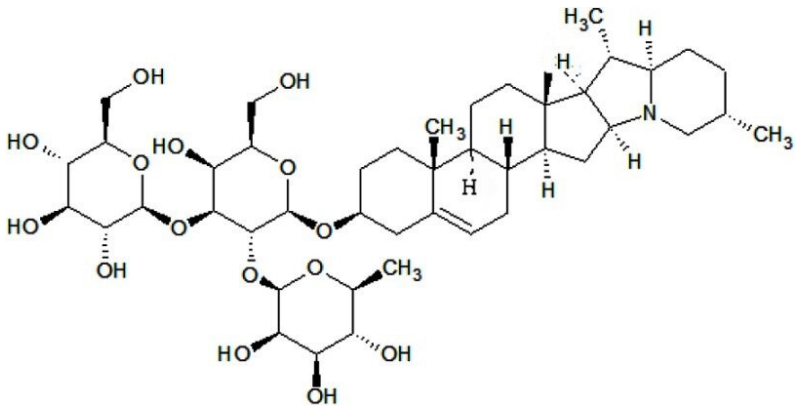

Figure 1.3: Molecular structure of BP.

Additionally, through pyrolysis, BPs can be converted into biochar. The biochar is greatly influenced by the temperature during pyrolysis; greater temperatures often result in increased surface area and porosity, which enhance adsorption efficiency (Patel et al., 2021).

The cellulose, hemicellulose, lignin, and pectin found in BPs give them a naturally occurring porous structure and a wide range of functional groups, including amine ($-NH_2$), carboxyl (-COOH), and hydroxyl (-OH) groups. Through processes including ion exchange, electrostatic attraction, and hydrogen bonding, these functional groups make it easier to interact with contaminants. (Lu et al., 2020). Table 1.3 shows the chemical constituent of dried BPs.

Table 1.3: Chemical composition of dried BP

Composition	**Percentage (%)**
Cellulose	67.6
Hemicellulose	45.6
Lignin	23.4
Pectin	15.89-24.08

Source: Nyong et al (2024), Khamsucharit et al (2017)

1.6 Objectives

The aims of the project are:

1. To study the efficiency of BP in removal of CIP from aqueous medium.
2. To validate the factors that may affect the efficiency of BP such as initial CIP concentration, pH, contact time, agitation rate, and adsorbent dosage.
3. To perform characterization studies on BP by using Fourier Transform-Infrared Spectroscope (FT-IR), Scanning Electron Microscope (SEM), and Atomic Force Microscope (AFM).
4. To determine the adsorption kinetics and isotherms model that can be used to explain the adsorption of CIP onto BP.
5. To study the influential factors using Plackett-Burman Design (PB) and obtain the optimized condition equation between the interactions among the factors using Response Surface Methodology (RSM).

CHAPTER 2

LITERATURE REVIEW

Thomas Graham conducted a more thorough investigation of the idea of adsorption in the 19th century after Carl Wilhelm Scheele made the initial observation of it in 1773 (Gregg & Sing, 1997). Irving Langmuir created the first quantitative model for adsorption on solid surfaces and established the formal theory between 1916 and 1918 (Langmuir, 1918). Adsorption refers to the process by which atoms, molecules, or ions from a gas, liquid, or dissolved solid accumulate on the surface of a material, forming a thin layer due to surface interactions. In contrast to absorption, which occurs when a material diffuses into its bulk, adsorption occurs only on the surface and is fuelled by intermolecular forces including chemical bonds etc (Sing, 1982). According to Ruthven (1984), there are two primary categories of adsorption: chemisorption, which involves stronger, frequently irreversible chemical connections, and physisorption, which involves weak, reversible physical forces. The process is governed by various factors, such as temperature, pressure, surface area, and the specific characteristics of both the adsorbent and the adsorbate. To quantitatively characterize adsorption behaviour, classical models like the Freundlich and Langmuir isotherms are frequently employed.

Adsorption is easier, less expensive, creates fewer secondary contaminants, and permits the reuse of adsorbents than traditional water treatment techniques such chemical precipitation and membrane filtration. With its high efficiency,

even at low contamination levels, it is a potential method for removing colors, heavy metals, and organic pollutants from water.

This chapter presents an in-depth review of recent advancements in adsorption technologies for effectively eliminating antibiotic waste, heavy metals, and dyes from aqueous environments. The main goal is to showcase the most recent findings in the creation and use of adsorbents, including both commercial and affordable, environmentally friendly substitutes. Activated carbon derived from biomass, industrial byproducts, agricultural leftovers, and other natural materials are examples of these alternative adsorbents. They offer cost-effective, environmentally friendly ways to remove antibiotic waste, which could enhance wastewater treatment plants' sustainability and performance.

2.1 Adsorbents

2.1.1 Activated Carbon (AC)

Activated carbon is widely used for adsorption processes due to its exceptional surface properties, including a high surface area, extensive porosity, and numerous functional groups that enhance its ability to attract and hold various contaminants (Bansal & Goyal, 2005). Due to its high porosity, which provides a lot of adsorption sites, it is very effective at eliminating pollutants from aqueous solutions, including chemical compounds, dyes, heavy metals, and even some microbes (Dias et al., 2007). Moreover, activated carbon is a cost-effective choice because it can be made from cheap and plentiful resources including coal, wood, and coconut shells (Ioannidou & Zabaniotou, 2007). Its appeal is further

influenced by its chemical stability, regeneration-based reusability, and capacity to work well throughout a broad pH and temperature range (Gupta et al., 2012). Activated carbon is favored in industrial, municipal, and environmental water treatment processes because of its significant advantages, making it one of the most employed adsorbents.

The presence of a range of functional groups on the surface of activated carbon, including hydroxyl (-OH), carboxyl (-COOH), carbonyl (C=O), and phenolic groups, makes it extremely successful in adsorption processes from the standpoint of functional groups. These groups increase the carbon surface's reactivity through hydrogen bonding, electrostatic attraction, and π-π interactions, leading to stronger interactions with various contaminants (Boehm, 1994). The kind and presence of what type of functional helps to determinine the adsorption capacity, selectivity, and efficiency, especially when dealing with polar molecules and heavy metal ions (Moreno-Castilla, 2004). Activated carbon is very adaptable for targeted pollutant removal because surface functionalization can be customized using chemical activation or modification treatments to improve certain adsorption capabilities (Li et al., 2003).

By creating activated carbon from coffee waste, Naganathan et al. (2021) aims to create a sustainable adsorbent that can remove CIP from water. To increase the coffee residue's porosity, surface area, and availability of functional groups and make it more efficient in adsorbing antibiotic molecules, they employed chemical activation.

They studied the adsorption of CIP onto coffee residue-based activated carbon under different conditions. The pseudo-second-order model of adsorption kinetics demonstrated that chemisorption, which involves electron exchange or

sharing between CIP molecules and the adsorbent surface, is the dominant mechanism controlling the process. It matches Langmuir isotherm, indicating that CIP formed a monolayer on a uniform surface. In their study, the maximum adsorption capacity (q_m) value is 105 mg/g.

Figure 2.1 illustrates the SEM results, demonstrating the high porosity that aids the adsorption process. The adsorption mechanisms identified, as supported by the FTIR spectra (Figure 2.2), involve hydrogen bonding between functional groups like hydroxyl and carboxyl groups between the negatively charged sites on the activated carbon and the cationic form of CIP. The significant affinity between the CIP and coffee-based carbon compounds was a result of these combined effects.

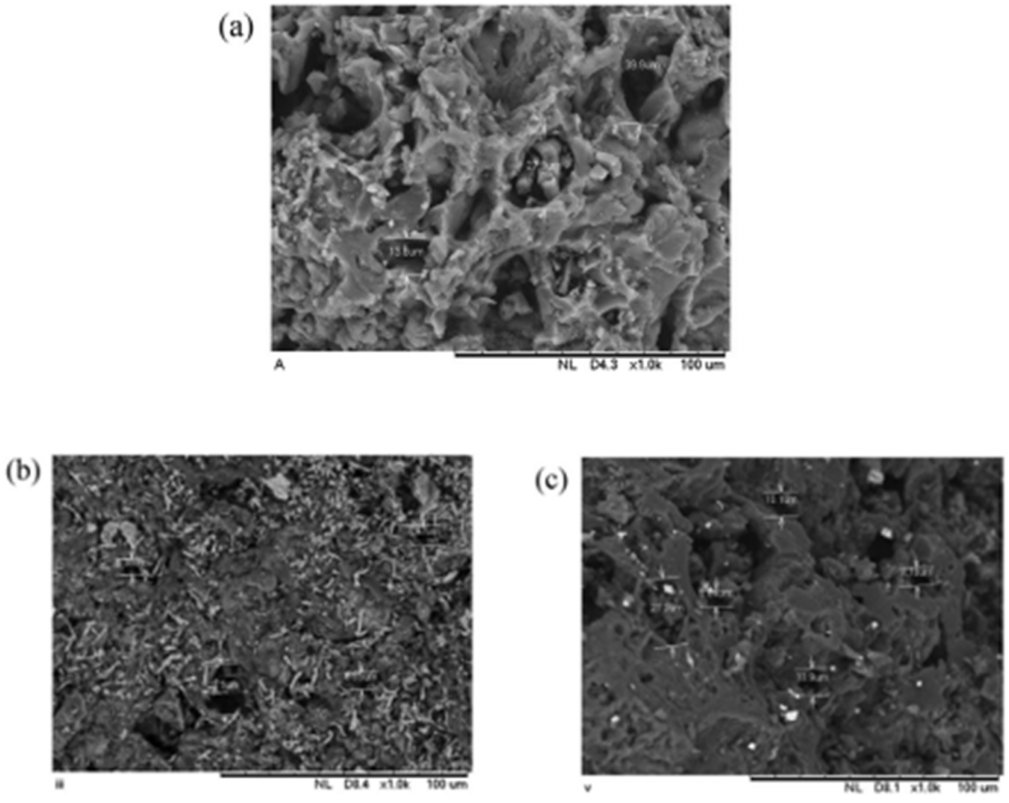

Figure 2.1: SEM images of activated carbons; (a) AC-CoR I, (b) AC-CoR II, and (c) AC-CoR III.

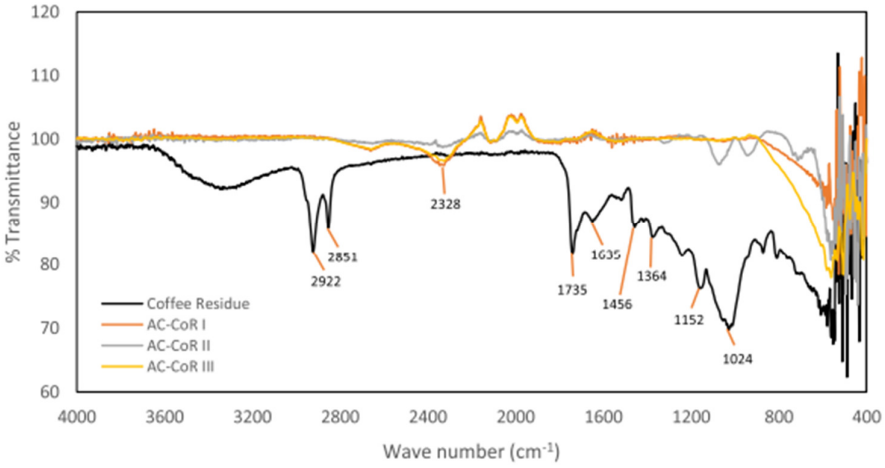

Figure 2.2: FTIR spectra of coffee residue and its activated carbon derivatives.

Liu et al. (2023) concentrate on the two-step activation process with potassium hydroxide (KOH) to produce high-performance activated carbon from peony seed shells. The resultant activated carbon's adsorption capacity was greatly increased by its extraordinarily large specific surface area of 2,980.96 m^2/g. The substance showed an outstanding adsorption capacity of 782.3 mg/g for CIP. The conformity of the adsorption process to the Langmuir isotherm model suggests that the adsorption sites on the surface are evenly distributed, and the CIP molecules are adsorbed onto the surface in a monolayer fashion.

The use of rice husk-derived biochar to extract CIP from water is being studied by Arun & Maharathi (2019). Rice husk was heated to 300°C to create the biochar, and the findings demonstrated a high removal efficiency of 96% of CIP in just 90 minutes. The agreement of the adsorption process with the Freundlich isotherm model implies multilayer adsorption on a heterogeneous surface, suggesting that the biochar's surface is varied and offers a range of adsorption sites. Furthermore, the pseudo-second-order model describes the adsorption process's kinetics, suggesting that the chemical interactions between the CIP

molecules and the biochar regulate the adsorption rate. This study demonstrates the possibility of biochar made from rice husks as an efficient and reasonably priced method of eliminating antibiotics from tainted water.

2.1.2 Agricultural Wastes

To improve the material's capacity to adsorb pollutants from water, several procedures are used to transform raw agricultural waste into effective adsorbents. Although rich in carbon and organic compounds, agricultural wastes including rice husks, corn cobs, coconut shells, and fruit peels need to be treated to fully realize their potential as adsorbents. Physical activation and chemical activation are the two main techniques usually used for the alteration.

To further maximize its adsorption potential, agricultural waste might further go through surface functionalization after activation. This can include grafting with additional chemical agents that enhance the material's interaction with target contaminants, modification with surfactants, or impregnation with metal salts or polymers.

According to the Li et al. (2018), peanut shells shown a strong ability to adsorb antibiotics from aqueous solutions, particularly CIP and tetracycline. Under ideal circumstances, the maximal adsorption capacity for CIP and tetracycline was about 91.68 mg/g and 72.51 mg/g. Adherence to Langmuir isotherm model indicated that adsorption process involved monolayer coverage on a surface and it aligns with pseudo-second order kinetic model.

The SEM images are shown in Figure 2.3. The peanut shells' surface showed a rough, uneven structure with lots of pores and voids, according to the SEM pictures. These structural characteristics probably help to explain the peanut shells' high adsorption capability since they give antibiotic molecules a lot of surface area to interact with. In Figure 2.4, the FTIR results revealed clear shifts in the absorption peaks, suggesting that the hydroxyl, carbonyl, and amine groups were essential to the adsorption process. These functional groups enable interactions with antibiotic molecules, including electrostatic interactions, hydrogen bonding, and potentially van der Waals forces. These results further reinforce peanut shells' promise as an inexpensive and efficient adsorbent in water treatment applications by confirming that their surface chemistry plays a role in their capacity to adsorb antibiotics from water.

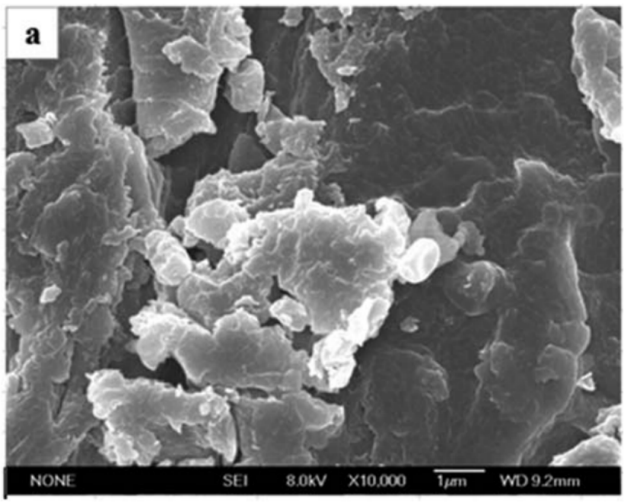

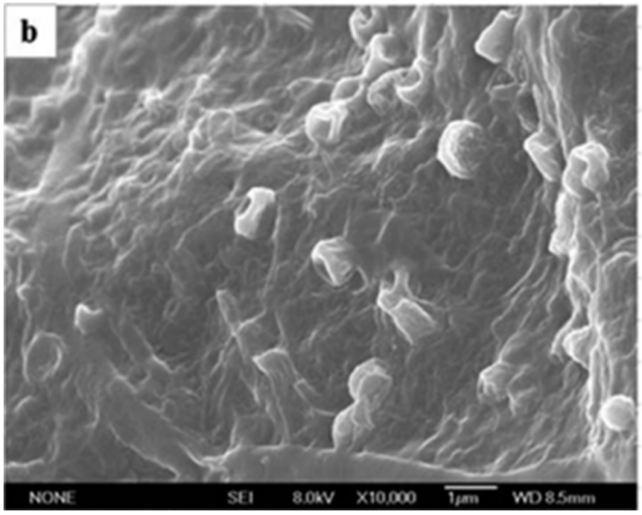

Figure 2.3: SEM micrograph images of peanut shells before (a) and after (b) antibiotic adsorption.

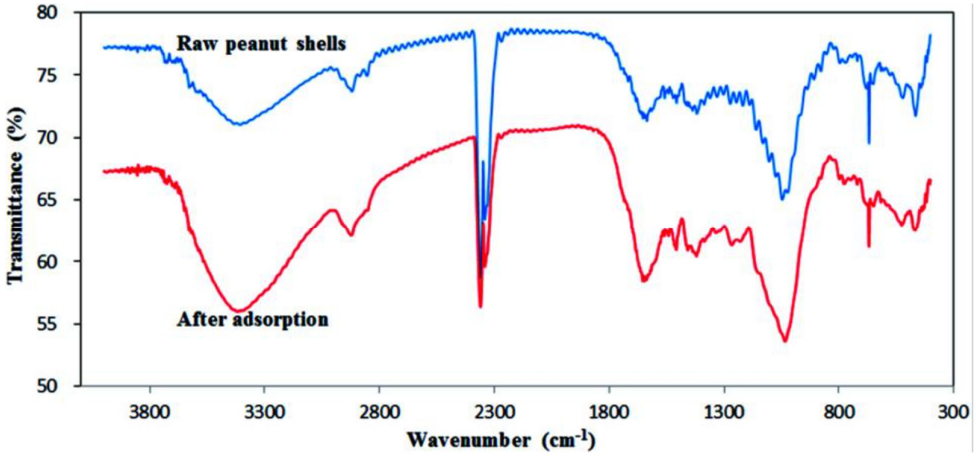

Figure 2.4: FTIR spectra of the peanut shells before and after antibiotic adsorption.

In their 2025 study, Abudu et al. explored the potential of raw sawdust as an adsorbent for eliminating the antibiotic rifampicin from aqueous solutions. It indicated that sawdust effectively removed rifampicin, reaching a peak removal efficiency of 65% when the adsorbent dosage was 31.3 g/L. Higher temperatures

were shown to enhance the spontaneous adsorption process, indicating physisorption as the predominant mechanism. Furthermore, the surface of raw sawdust was rough, as shown by the SEM images; however, its surface became smoother after acid treatment, which probably improved the adsorption process by upsetting the lignin structure. As a practical water purification method, it shows that raw sawdust, especially when processed, can be used as an inexpensive, sustainable material to remove antibiotics from water.

2.1.3 Biosorbents

Natural or modified substances originating from biological sources, known as biosorbents, have the capacity to remove pollutants from aqueous solutions, including organic pollutants, dyes, and heavy metals. Since these materials are usually made from industrial byproducts, agricultural waste, or even microorganisms, they offer an affordable and environmentally friendly substitute for traditional adsorbents such synthetic resins and activated carbon (Filote et al., 2021). Due to their great effectiveness, biodegradability, and low environmental impact, biosorbents have drawn a lot of interest for application in environmental remediation (Gupta et al., 2015). Functional compounds like hydroxyl, carboxyl, and amino groups that are present on the surface of the biosorbent participate during the adsorption process (Volesky & Holan, 1995). These groups help the pollutants bind through processes including ion exchange, hydrogen bonding, and electrostatic attraction.

Chitosan, a biopolymer derived from chitin, has gained significant attention because of its effective adsorption capabilities in removing a variety of substances, including antibiotics, from aqueous solutions. Chitosan's popularity stems from its biodegradability, non-toxicity, and functional groups like amine and hydroxyl groups that facilitate interactions with contaminants. Due to these functional groups, chitosan-based adsorbents have high adsorption capabilities, which makes them appropriate for environmental remediation, especially in water treatment applications. Additionally, because of its adaptability, chitosan may be modified by processes like grafting and crosslinking to improve its stability and adsorption capacity (Filote et al., 2021).

Bui et al. (2023) discovered that chitosan-magnetite composites (CS-MNPs) were very successful in eliminating CIP and levofloxacin, two fluoroquinolone drugs, from aqueous solutions. Pseudo-second order kinetics and the Langmuir isotherm model characterized the adsorption behaviour, indicating monolayer adsorption, while removal efficiencies surpassed 98% for both antibiotics in separate solutions. The competitive Langmuir model explained the adsorption in binary systems, where the adsorption of one antibiotic was diminished by the presence of the other. Additionally, it showed that CS-MNPs could be efficiently regenerated and reused, with removal efficiencies of roughly 64.98% and 59.56% for CIP and levofloxacin, respectively, maintained after four cycles. The composites demonstrated over 98% removal efficiency in actual water samples, demonstrating their usefulness in treating fluoroquinolone antibiotic-contaminated water.

The FTIR spectra (Figure 2.5) displayed distinctive peaks that corresponded to the hydroxyl and amine groups of chitosan, which oversee interacting with the

antibiotics. The emergence of certain peaks associated with iron-oxide linkages in the composite material validated the magnetite addition. The changes in peak positions and intensities observed after the adsorption of fluoroquinolone antibiotics proves the participation of functional groups in the process. FTIR analysis verified that chitosan-magnetite composites effectively adsorb antibiotics from aqueous media, with electrostatic interactions and hydrogen bonding being key in the uptake of CIP and levofloxacin.

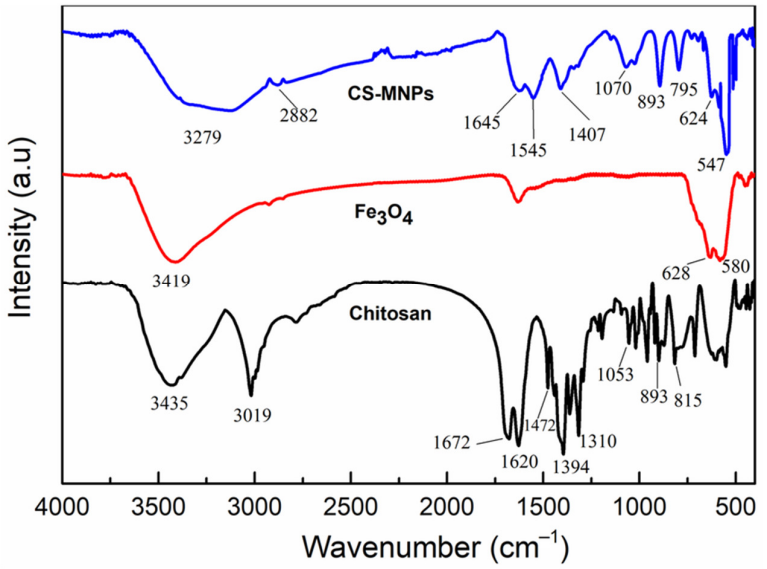

Figure 2.5: FTIR spectra of CS, MNPs, and CS-MNPs.

2.2 Adsorbates

2.2.1 Antibiotics

Excellent removal performance was revealed by the work of Mostafapour et al. (2021) in examining the adsorptive removal of amoxicillin utilizing a magnetic graphene oxide nanocomposite. According to Langmuir isotherm fitting, the

nanocomposite's highest adsorption capacity (q_m) was 312.5 mg/g, demonstrating a potent and effective adsorption capability. The strong correlation ($R^2 > 0.99$) with the pseudo-second-order model confirmed that chemisorption was the primary mechanism controlling the adsorption process. The Langmuir constant (K_L) of 0.042 L/mg confirmed that it is more appropriate than the Freundlich model for the isotherms, validating the process of monolayer adsorption.

Yadav et al. (2022) examined the application of chemically activated waste tea trash as a sustainable and cost-effective adsorbent for eliminating tetracycline (TC) from water. To increase the tea waste's surface area, porosity, and adsorption capacity, two activation techniques were used: sulfuric acid (H_2SO_4) and phosphoric acid (H_3PO_4). The excellent fit ($R^2 > 0.99$) to pseudo-second-order kinetics confirms that chemisorption is the primary mechanism controlling the process. The Langmuir isotherm model, which indicates monolayer adsorption on a uniform surface, most accurately represents the equilibrium data. Sulfuric acid activation marginally surpassed phosphoric acid activation, as evidenced by the maximum adsorption capabilities of 186.5 mg/g for H_2SO_4-activated tea waste and 172.8 mg/g for H_3PO_4-activated tea waste. Table 2.1 illustrates the comparative studies on the adsorptive removal of antibiotic wastes using cellulose-based adsorbents.

Table 2.1: Adsorption of antibiotic wastes by cellulose-based adsorbents.

Adsorbent	Adsorbate	Maximum adsorption capacity (mg/g)	References
Wheat Straw (AWS)	Ciprofloxacin	14.51	(Alawa et al., 2025)
Rice Straw Biochar	Ciprofloxacin	131.58	(Adegoke et al., 2023)
Rice Husk Biochar	Azithromycin	612.22	(Ajala et al., 2023)
Corn Stalk Biochar	Tyrosine Antibiotics	14.4	
Guayule Bagasse Biochar	Erythromycin	17.12	

2.2.2 Heavy metals

The toxicity, resilience, and potential for bioaccumulation in living organisms make heavy metals in water a major ecological hazard. Water supplies are frequently contaminated with metals like lead (Pb), cadmium (Cd), mercury (Hg), arsenic (As), and chromium (Cr), which enter through mining operations, industrial effluents, agricultural runoff, and improper waste management practices. These metals can cause major health hazards to aquatic ecosystems and

people, including cancer, developmental disorders, and organ damage, even at low doses.

To eliminate heavy metals wastewater, Gargiulo et al. (2024) assesses the utilization of rice husk activated carbon (RhAC) and its composite with polyvinylpyrrolidone (PVP). They combined RhAC with PVP to improve its adsorption capabilities. Tests were conducted on the adsorption capabilities of RhAC and the RhAC-PVP composite for cadmium (Cd^{2+}), lead (Pb^{2+}), and chromium (Cr^{3+}).

According to the findings, RhAC and its PVP composite shown notable adsorption capabilities for the elimination of these heavy elements. The RhAC-PVP composite exhibited a higher adsorption capacity than RhAC alone, demonstrating that PVP improved the material's performance. The RhAC-PVP composite had the highest effectiveness in removing lead and chromium, obtaining adsorption values of approximately 85 mg/g for Pb^{2+} and 90 mg/g for Cr^{3+}. Equilibrium tests were used to estimate the q_m for the metals.

X-ray diffraction (XRD) investigation (Figure 2.6) demonstrated the crystalline structure of RhAC and its composite with PVP. The patterns displayed clear peaks, indicating that the rice husk was successfully activated and that the composite was formed. Following activation, variations in peak intensities suggested improved surface characteristics, which are critical for enhancing heavy metal adsorption.

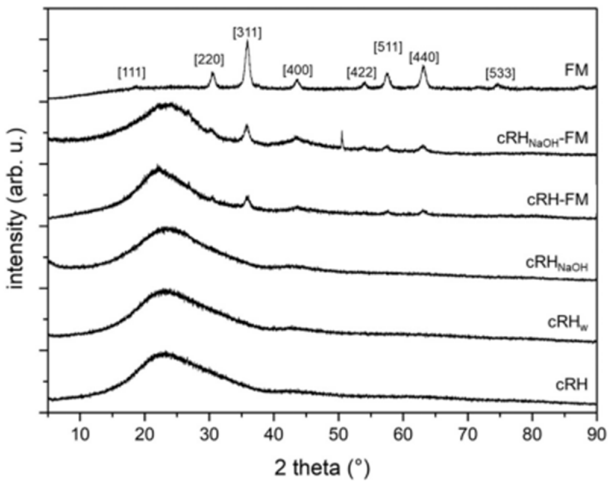

Figure 2.6: XRD patterns of the materials.

Hydroxyl (-OH), carboxyl (-COOH), and carbonyl (C=O) were detected on the surface of RhAC and its composite with PVP by Fourier-transform infrared (FTIR) analysis (Figure 2.7). These functional groups play a crucial role in helping heavy metals like lead, chromium, and cadmium bind to the adsorbent, improving its capacity to extract these pollutants from wastewater.

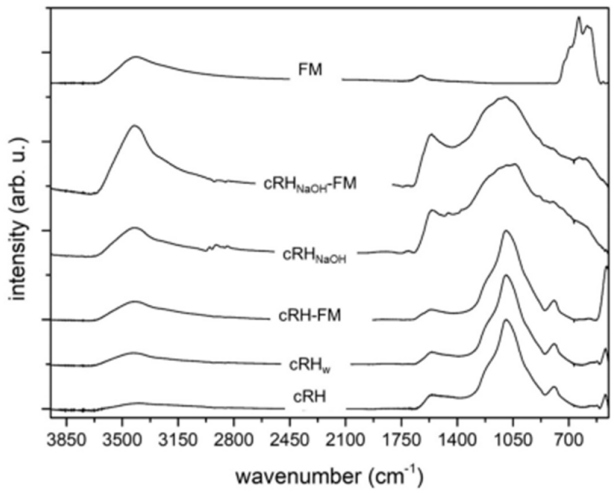

Figure 2.7: FTIR spectra of the materials acquired on KBr pellets in the 500–3900 cm^{-1} range.

The utilization of leftover coffee grounds as adsorbents to extract heavy metals from aqueous solutions was examined by Wu et al. (2016). To improve its adsorption properties, the coffee waste underwent processing and characterization. According to experimental findings, discarded coffee dregs were successful in extracting metals from water, including copper (Cu^{2+}), cadmium (Cd^{2+}), and lead (Pb^{2+}).

Heavy metals as Pb^{2+}, Cd^{2+}, and Cu^{2+} were efficiently adsorbed from water by waste coffee residues. Adsorption suggested chemisorption and the data was best represented by the Langmuir isotherm model, which provided q_m values of 87.5 mg/g for Pb^{2+}, 72.4 mg/g for Cd^{2+}, and 65.1 mg/g for Cu^{2+}.

Figure 2.8 shows the SEM results of the discarded coffee dregs which had an uneven, rough, and porous surface—all characteristics that are perfect for adsorption. The SEM pictures revealed clear alterations following heavy metal adsorption, with metal ions clearly adhered to the surface and certain pores looking obstructed. The FTIR analysis (Figure 2.9) revealed the presence of functional groups like carbonyl (C=O), carboxyl (-COOH), and hydroxyl (-OH) in discarded coffee dregs. These functional groups' role in binding metal ions was confirmed by shifts and intensity variations seen following heavy metal adsorption.

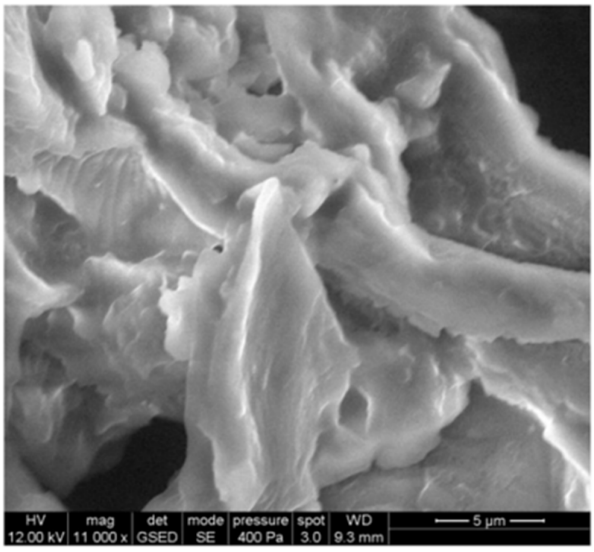

Figure 2.8: SEM micrograph of WCRs.

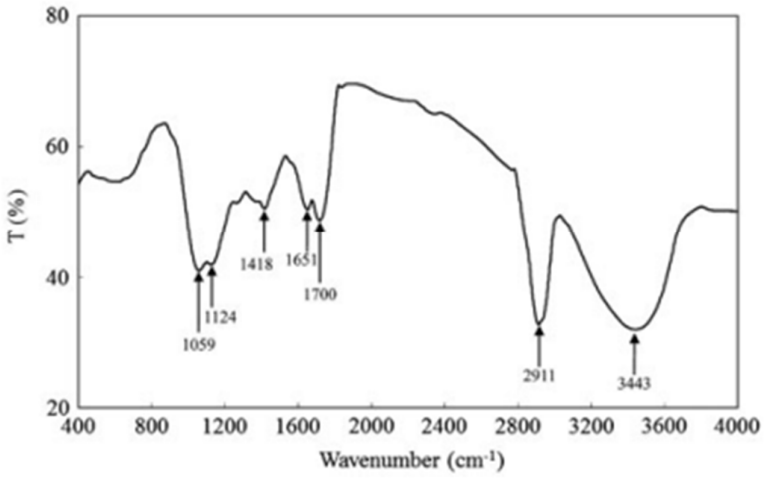

Figure 2.9: FTIR spectra of WCRs.

Shan et al. (2020) investigated both single-metal and competitive heavy metal adsorption onto peanut shell biochar. Peanut shells were used to make the biochar, which was then tested for adsorption capabilities. The q_m for copper (Cu^{2+}), cadmium (Cd^{2+}), and lead (Pb^{2+}) in single-metal systems were determined to be 88.3 mg/g, 95.8 mg/g, and 112.5 mg/g, respectively, according to the Langmuir isotherm model. The pseudo-second-order model predicted by the

adsorption kinetics ($R^2 > 0.99$) points to chemisorption as the primary process. The presence of several metal ions in competing adsorption systems somewhat reduced the adsorption capabilities; nonetheless, peanut shell biochar continued to exhibit a greater affinity for Pb^{2+} than for Cd^{2+} and Cu^{2+}. FTIR analysis (Figure 2.10) verified that the binding of the metal ions was facilitated by functional groups such as carboxyl (-COOH) and hydroxyl (-OH).

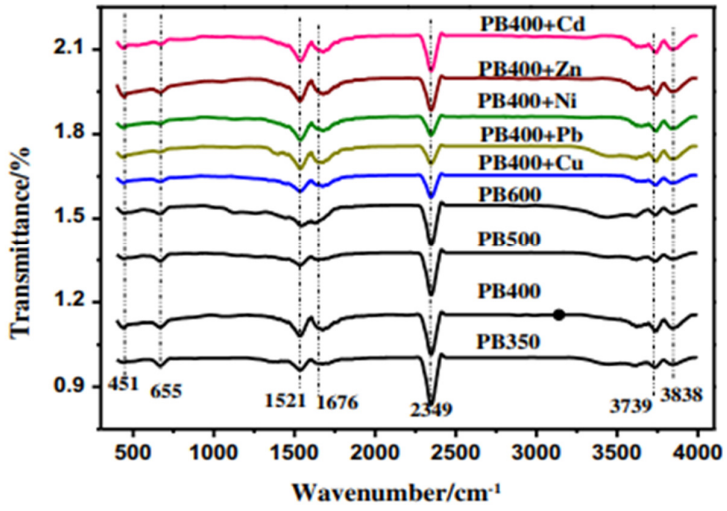

Figure 2.10: FTIR spectra of PBC350, PBC400, PBC500, PBC600, and PBC400 after heavy metal adsorption.

2.2.3 Dyes

Dyes released from the paper, plastics, and textile industries represent a significant source of water pollution due to their high toxicity and persistence in aquatic environments. They damage aquatic life, block sunlight, and lower oxygen levels when released into water bodies without being properly treated, posing a major threat to the environment. Numerous colors are harmful, non-

biodegradable, and can cause cancer and skin irritation in people. To safeguard ecosystems and public health, dyes must be eliminated from wastewater.

Andrade Siqueira et al. (2020) explores the adsorption of Methylene Blue (MB) dye by sugarcane bagasse (SCB). When the biomass was examined with scanning electron microscope, the surface morphology of SCB was discovered to be rough and porous, making it perfect for dye adsorption. (Fig.2.11)

Batch adsorption experiments were conducted with different dye concentrations, pH levels, and contact time. It follows the pseudo-second order kinetic model. The model indicates that the adsorption rate is primarily governed by chemisorption, with adsorption sites being occupied according to a second-order reaction mechanism. The good agreement between the Langmuir isotherm model and the equilibrium adsorption data suggests that the adsorption process takes place on a monolayer surface with identical, homogeneous adsorption sites. The study determined the q_m was 43.75 mg/g for MB.

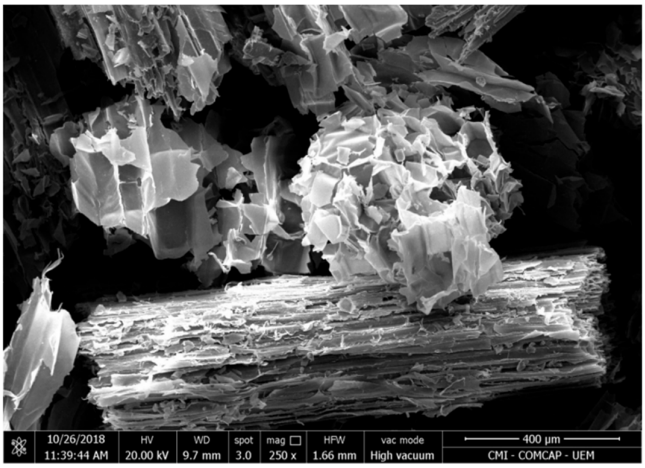

Figure 2.11: SEM micrograph of general view of the sample of sugarcane bagasse (SCB), showing fibres and residues with 250× magnification.

Sangeetha Piriya et al. (2021) examines the adsorption of Malachite Green (MG) colour by coconut shell carbon activated by zinc chloride. It showed that at a dye concentration of 100 mg/L, activated carbon had a q_m of 90.5 mg/g for MG, reaching equilibrium after 120 minutes. Adsorption results fit the Langmuir isotherm model well, confirming monolayer adsorption, and the process followed pseudo-second-order kinetics, indicating chemisorption.

Ertaş et al. (2010) explore the potential of using cotton-based materials, including cotton dust, waste, and stalks, to remove Methylene Blue (MB) dye from aqueous solutions through adsorption. The findings showed that cotton stalks were the most effective adsorbent of the three materials, when compared to cotton waste and cotton dust. The q_m of cotton stalks was found to be 72.5 mg/g. It obeys the pseudo-second-order kinetics, implying that chemical bonding between the dye molecules and the adsorbent surface controls the rate of the reaction.

2.3 CIP as Adsorbate

Patel et al. (2021) looks at the adsorptive removal of acetaminophen and CIP from aqueous solutions using biochars made from BPs. The biochars were made by pyrolysis at temperatures between 450°C and 750°C. The biochar made at 750°C had the highest CIP adsorption capability, reaching 23.3 mg/g at a starting temperature of 10°C. The authors concluded that variables including pH, particle size, adsorbent dosage, and starting concentration all had an impact on adsorption performance. The adsorption process exhibited pseudo-second-order kinetic behaviour, indicating that the rate-limiting step involved chemisorption. It aligns with Langmuir isotherm, affirming monolayer adsorption on a homogeneous surface.

According to the SEM pictures (Figure 2.12), the biochar's surface had rough, uneven textures and was extremely porous, offering a lot of surface area for adsorption. The physical adsorption process was confirmed when the charcoal surface became more congested with deposited dye molecules following the CIP adsorption. The CIP adsorption on the biochar surface was evident from the increased surface roughness, showing that the material underwent clear morphological changes.

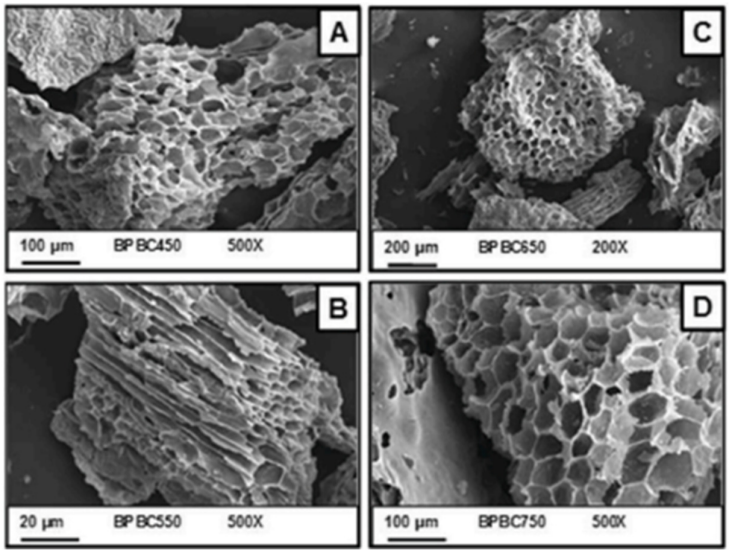

Figure 2.12: SEM micrographs (A–D) of the developed biochars.

Several important functional groups were present in the FTIR spectra (Figure 2.13) both before and after adsorption. The hydroxyl (-OH), carbonyl (C=O), and carboxyl (COOH) groups that cause CIP to adsorb were represented by distinctive peaks in the biochar prior to adsorption. The appearance of new peaks after CIP adsorption suggested chemical binding on biochar surface. This implies that by creating ionic contacts or hydrogen bonds with the CIP molecules, functional groups like hydroxyl and carboxyl are essential to the adsorption process.

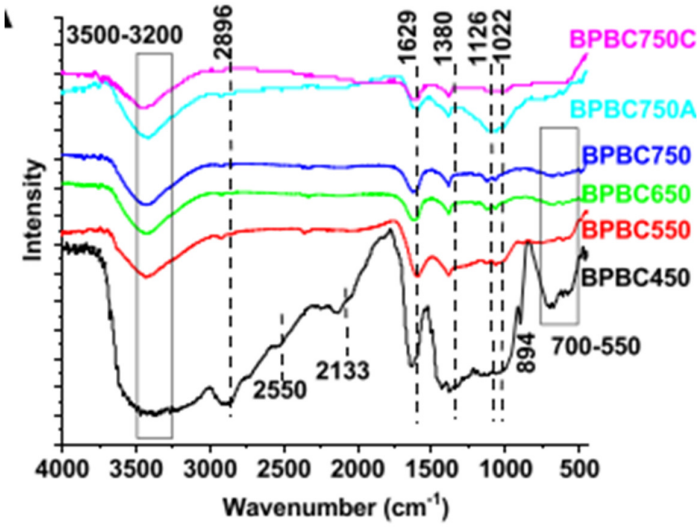

Figure 2.13: FTIR spectras of BP biochars (BPBC450, BPBC550, BPBC650 and BPBC750) along with BPBC750 after CIP (BPBC750C) and acetaminophen (BPBC750A) adsorption.

Karim et.al. (2024) explored the application of BP-based activated carbon (BPAC) for CIP removal from aqueous solutions. The BPAC was produced using pyrolysis, followed by adsorption tests under varying conditions to determine its optimal properties. It was discovered that BPAC's highest adsorption capacity for CIP was 96.7% removal effectiveness when 200 mg of activated carbon were used. The ideal adsorption conditions included a pH of 6, a 120-minute contact time, and an initial CIP concentration of 50 mg/L. The analysis of the adsorption kinetics was conducted using both linear and nonlinear models. The nonlinear method produced a significantly better fit, which implies that the adsorption process is influenced by a more intricate and complex mechanism than was initially considered.

According to the SEM pictures (Figure 2.14), the BPAC's surface was rough and porous, with many imperfections and voids. These features increase the

material's surface area and adsorption capacity. CIP adsorption caused the surface to become more clogged, as indicated by increased roughness and fewer visible pores. The observed morphological change suggests that CIP molecules were successfully captured by the BPAC surface, filling the pores and adhering to it. This implies that BPAC is an effective aqueous solution contaminant remover. Apart from the studies mentioned, Table 2.2 shows the list of other studies on the adsorptive removal of CIP.

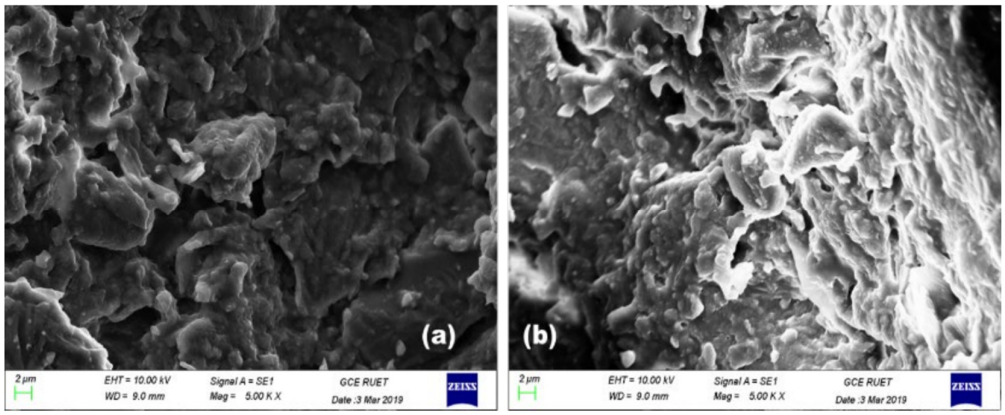

Figure 2.14: SEM of BPAC before (a) and after adsorption (b).

Table 2.2: Adsorption of CIP by BP adsorbents and other adsorbents.

Adsorbent	Adsorbate	Maximum Adsorption Capacity (mg/g)	References
Banana Stalk	Ciprofloxacin	49.7	(Agboola & Bello, 2020)
Banana Peel Biochar	Ciprofloxacin	9.2	(Patel et al., 2021)
Banana peel biochar-supported $NiFe_2O_4$ nanocomposite	Ciprofloxacin	63.29	(Azzam et al., 2023)
CeO_2/Palygorskite Hybrid Material	Ciprofloxacin	15.0	(Campos et al., 2024)
Surfactant-Modified Sepiolite (SMS)	Ciprofloxacin	63.84	(Balarak et al., 2022)

CHAPTER 3

MATERIALS AND METHODOLOGY

3.1 Chemicals and Reagents

Table 3.1: Chemicals and Reagents used in the project.

Chemicals/Reagents	Manufacturer
Hydrochloric Acid	AnalaR NORMAPUR
Sodium Hydroxide	Merck KGaA
Ciprofloxacin	ACROS ORGANICS

3.2 Adsorbent Preparation

The BPs came from a Kampar, Perak, banana fritters stand. The collected BPs were sliced into smaller pieces. The BPs were rinsed with tap water and washed with distilled water to remove dirt and contaminants. The peels were heated at 60°C for the entire night. Then, it was grounded into a powder. For the aim of decolorizing, the powdered BPs were steeped in distilled water at 60°C with periodic stirring. The decolorization procedure was carried out five times. The powder was then dried once more for a full day. The resulting BPs were passed through a 1 mm sieve. The dried BPs were then sealed in a plastic bag for future use in experiments.

3.3 Adsorbate Preparation

CIP was used as the adsorbate throughout the whole project. CIP is a broad-spectrum fluoroquinolone antibiotic that is extensively utilized in clinical practice to treat infections. It is classified as a second-generation fluoroquinolone with the molecular formula $C_{17}H_{18}FN_3O_3$ and a molecular weight of approximately 331.34 g/mol.

A 0.5 L of CIP with 500 mg/L (ppm) was prepared for the whole project. It was diluted with distilled water and kept in the dark. Further dilutions were needed for subsequent batch experiments.

3.4 Batch Experiment Studies

In each batch adsorption test, 0.05 grams of BP powder were introduced into 25 mL of a 25 mg/L CIP solution contained within a 50 mL centrifuge tube. To guarantee homogeneity, the tube was set on an orbital shaker and agitated for 2 hours at 150 rpm and standard room temperature (stp), unless otherwise noted. Two trials of each study step were carried out, and the average of the outcomes was noted. In addition, control experiments were performed without BP powder to ensure that CIP adsorption takes place on the BP material itself and not on the walls of the centrifuge tube.

The absorbance of the CIP solution's supernatant was then determined through UV-Vis spectrophotometer after the centrifugation. The wavelength at which the greatest absorption takes place, 276 nm, was used to record the absorbance of every sample. The initial and final concentrations of the CIP

solution were determined by applying the formula derived from the calibration curve, as outlined in Appendix A. The following equation was used to determine the percentage uptake of CIP:

$$Percentage\ uptake\ of\ CIP\ (\%) = \frac{C_0 - C_t}{C_0} \times 100\% \qquad \textbf{[1]}$$

Where, C_0 = Initial concentration of CIP solution (mg/L)

C_t = Concentration of CIP at time, t (mg/L)

3.4.1 Effect of Contact Time

For examining the effect of contact time, 0.05 g of BP was mixed with 25 mL of CIP solutions at three different concentrations: 10, 25, and 50 mg/L. The mixtures were then agitated on the orbital shaker at a fixed speed of 150 rpm. To evaluate how exposure duration affects adsorption effectiveness across different CIP concentrations, the experiments were carried out at 5, 10, 15, 30, 60, 120, and 180 minutes.

3.4.2 Effect of Initial Concentration of CIP

Three working solutions with the concentrations of 10, 25, and 50 mg/L were used for evaluating the impact of CIP concentration on the adsorption process. For each concentration, 25 mL of CIP solutions were put in centrifuge tubes with 0.05 g of After that, the samples were set up onto an orbital shaker and taken out for examination at certain time intervals.

3.4.3 Effect of Adsorbent Dosage

To assess the influence of BP powder dosage on CIP adsorption, varying amounts of BP (0.01, 0.02, 0.03, 0.04, 0.05, and 0.06 g) were introduced into a 25 mg/L CIP solution. Each combination was shaken for 2 hours at 150 rpm to assess the effect of different dosages on adsorption efficiency.

3.4.4 Effect of Agitation Rate

The impact of different speeds on CIP adsorption was investigated using an orbital shaker that was set to 50, 150, and 200 rpm. The experiments were carried out at the same intervals of time as the natural pH of CIP solution.

3.4.5 Effect of pH

CIP solutions with pH values between 2 and 10 were prepared. This was accomplished by adding varying quantities of sodium hydroxide (NaOH) and hydrochloric acid (HCl) dropwise. For each CIP solution with an adjusted pH, 0.05 g of BP powder was introduced into 25 mL of a 25 mg/L CIP solution.

3.5 Characterization Analysis

3.5.1 UV-Visible Spectroscopy

A Thermo Scientific GENESYS 50 UV/Vis spectrophotometer was used to monitor the absorbance of the supernatant from the CIP solution at predetermined intervals after the adsorption process. The wavelength of 276 nm, which is the maximum wavelength of the CIP in an aqueous medium, was used to monitor and record the absorbance measurements. This enables the accurate tracking of the CIP concentration remaining in the solution throughout the process.

3.5.2 Fourier-Transform Infrared Spectroscopy (FT-IR)

FTIR was used to identify the functional groups present in the BP both prior to and during the adsorption of CIP. Specifically, a Perkin Elmer Spectrum FX 1 model was used. The wavenumber range used for the analysis was 4000–400 cm^{-1}.

3.5.3 Scanning Electron Microscopy (SEM)

SEM was applied to thoroughly examine BP's surface morphology. A JEOL-JSM-6701 F model running at 4.0 kV of emission current was used for the analysis.

3.5.4 Atomic Force Microscopy (AFM)

AFM was used to investigate the BP's surface both before and after dye adsorption using the Park XE-70 AFM model. This method provided a detailed three-dimensional visualization of the surface features at the atomic level, enabling a thorough analysis of the morphological and textural changes associated with CIP adsorption.

CHAPTER 4

RESULTS AND DISCUSSIONS

4.1 Characterization Analysis

4.1.1 Fourier-Transform Infrared Spectroscopy (FT-IR)

FTIR was used to characterize the functional groups present in BP and determine any differences after the adsorption process. Figure 4.1 shows the structure of β-D-glucose. The main structural element that gives it stiffness is cellulose, a polysaccharide composed of glucose units that are made of β-D-glucose monomers, linked by β-(1→4)-linked glucose units. The IR spectrum offers important information about the chemical reactions and surface alterations that take place on the BP during the CIP adsorption process.

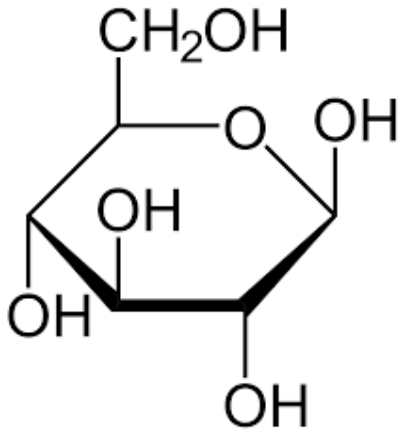

Figure 4.1: Structure of β-D-glucose.

There are several specific functional groups that are shown in the IR spectrum which are related to the structure. In Figure 4.2, the prominent and broad

peak at 3422 cm^{-1} suggests the presence of a free hydroxyl group (-OH). Since there are many hydroxyl groups in the structure, therefore it is the most intense peak. After the adsorption of CIP, the peak shifted, and its intensity increased to 3447 cm^{-1}, due to the strong interaction between the molecules in the aqueous medium, leading to the formation of hydrogen bonds.

Along with the hydroxyl group peak, small peaks at 2955 cm^{-1} and 2919 cm^{-1}, corresponding to C-H stretching vibrations of aliphatic C-H bonds in the cellulose structure, were observed. A slight shift from 2955 cm^{-1} to 2967 cm^{-1} indicates CIP interaction with the C-H bonds.

A medium peak at 1636 cm^{-1} was detected, which is contributed by the presence of a carbon-carbon double bond (C=C), signifying the existence of a conjugated alkene within the structure. There are no obvious changes of the peak which indicated that the carbon-carbon double bond is not likely participated in the adsorption process.

Alongside the C=C peak, multiple small peaks were observed at 1437 cm^{-1} and 1377 cm^{-1}. These peaks represent C-H bending vibrations, which point to the presence of methyl groups within the structure. Additionally, the peaks at 1246 cm^{-1} to 1036 cm^{-1} are the stretching vibrations of ether groups (C-O-C). These peaks showed obvious decrease in intensity which is due to the adsorption process of CIP.

4.1.2 Scanning Electron Microscopy (SEM)

SEM is a potent imaging method that may be used at high magnification to examine the surface morphology of materials. It operates by moving a concentrated electron beam across the surface of the sample, resulting in interactions that generate a variety of signals, including backscattered and secondary electrons. These signals offer comprehensive details about the material's texture, composition, and topography. The adherence of adsorbates to the adsorbent surface was confirmed through SEM, which allowed the visualization of structural changes prior to and following adsorption.

Figure 4.3 shows the SEM images of BP before and after CIP adsorption. The adsorption capacities of BP are significantly influenced by its very porous and fibrous surface shape as revealed by scanning electron microscopy analysis or images. Before adsorption (Figure 4.3a), the surface has ridges and grooves that are visible and gives the impression of being rough and uneven. After adsorption (Figure 4.3b), the ridges and grooves become saturated, and the surface is smoother than the image before adsorption. This indicated that the CIP molecules are covered and occupied the binding sites, which proven the presence of adsorption process.

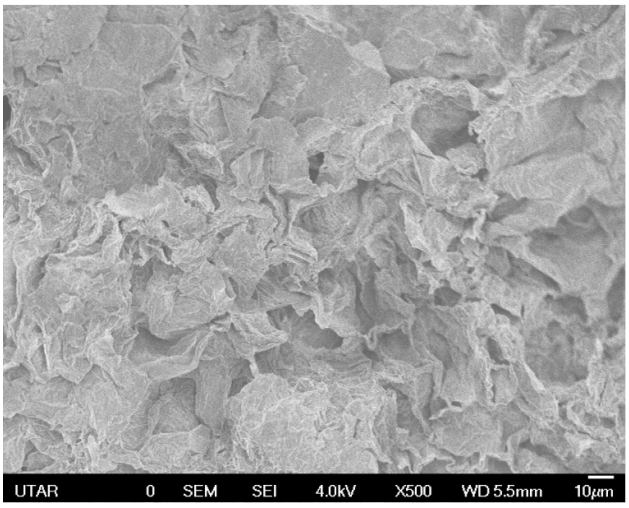

(a)

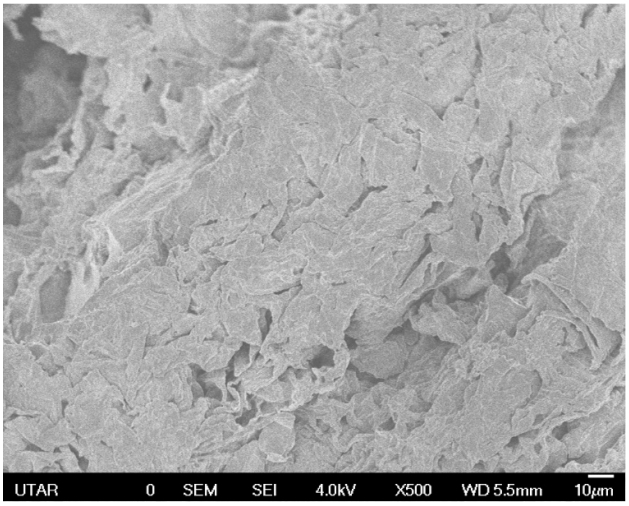

(b)

Figure 4.3: SEM image of BP before (a) and after (b) CIP adsorption (× 500 magnification).

4.1.3 Atomic Force Microscopy (AFM)

Atomic Force Microscopy (AFM) is a powerful tool for obtaining high-resolution images of surfaces, enabling detailed analysis at the atomic. This method involves measuring the forces between a sharp probe and the material as it traverses the

surface of the sample, enabling the generation of detailed topographical maps that provide insight into surface characteristics.

4.2 Batch Experiment Studies

4.2.1 Effect of Contact Time and Initial Concentration of CIP

Contact time and CIP concentration affect the adsorption process. As shown in the Figure 4.5, the adsorption efficiency of BP towards CIP increased steadily as the time was prolonged. Apart from that, it also demonstrated that when the concentration of CIP had increased, the removal efficiency decreased. The equilibrium time was determined at 2 hours, and the adsorption seemed to stop. In the first 30 minutes, the removal of CIP increased rapidly indicating the adsorption process of BP. However, the process slowed down gradually and achieved an equilibrium time of 60 minutes (1 hour). The process was monitored for another 120 minutes and 180 minutes to validate this statement. There is only a slight increase of percentage uptake between 60 minutes to 120 minutes, which fell in the range of 1.0 % to 2.0 %, indicated that the equilibrium time was 60 minutes.

Initially, the adsorption rate is high because of the abundant binding sites, but it gradually decreases as the sites become increasingly saturated (Hettithanthri et al., 2022). The adsorption process is affected by the initial concentration of CIP as well. A greater proportion of the antibiotic is eliminated at lower concentrations because there are more active sites accessible for adsorption. Nevertheless, BP's adsorption capacity rises with increasing concentrations, but as the adsorbent reaches saturation, the percentage removal efficiency falls (Magesh. et al., 2021).

4.2.2 Effect of Adsorbent Dosage

Figure 4.6 shows the percentage uptake of CIP by different dosages of BP. The dosage of the adsorbent is a crucial factor in the adsorption process, and thus, this parameter was thoroughly investigated. The amount of BP dosage studied was 0.01 g, 0.02 g, 0.03 g, 0.04 g, 0.05 g, and 0.06 g. In Figure 4.6, the bar chart highlights that a higher dosage corresponds to a greater removal percentage of CIP.

The percentage of the contaminant that was adsorbed likewise gradually rises, going from 34.92% at 0.01 g to 73.98% at 0.06 g. Since more surface area is available for interaction with the pollutant, this pattern supports the well-established idea that adsorption efficiency increases with higher adsorbent availability.

As more adsorbent is added, the efficiency of adsorption per unit mass may drop due to the saturation of available sites (Ahmaruzzaman, 2008). These saturation effects, where an excess of adsorbent can cause particle aggregation and a decrease in accessible active sites, have been extensively documented in adsorption studies (Balarak et al., 2021)

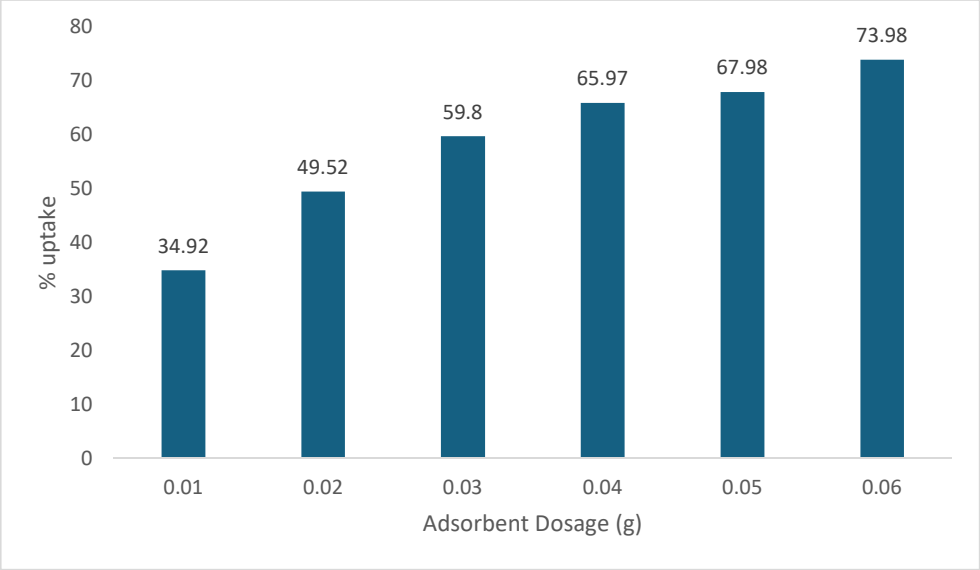

Figure 4.6: Effect of dosage of BP on the adsorption of CIP.

4.2.3 Effect of Agitation Rate

According to Figure 4.7, CIP adsorption increases rapidly at all agitation speeds during the first 20 minutes of the adsorption phase. The presence of numerous active sites on the surface of the banana peel and a greater concentration differential between the adsorbent and solution are responsible for this first phase (Patel et al., 2021). The sharp increase in the uptake % suggests that mass transfer was improved during this time.

The rate of adsorption slows and eventually plateaus over time, signalling the approach of equilibrium. Over the course of the operation, 200 rpm consistently exhibits the highest percentage absorption among the three agitation speeds, reaching roughly 73% at 180 minutes. This indicates that by decreasing the thickness of the boundary layer around the banana peel particles, increased

agitation promotes the diffusion of ciprofloxacin molecules into the active sites (Foo & Hameed, 2010). However, the 50 rpm system approaches equilibrium more slowly and attains a marginally lower maximum uptake, suggesting restricted mass transfer and potential adsorbent particle aggregation, which lowers the effective surface area (Wang & Zhu, 2007).

4.2.4 Effect of pH

Figure 4.8 presents a depiction of the adsorption behaviour of CIP on BP within the pH range of 2 to 10. The uptake rate of CIP showed a notable increase from 17.92% at pH 2 to 59.08% at pH 3. The trend continued to increase slowly until pH 9 at the maximum, followed by a decrease at pH 10.

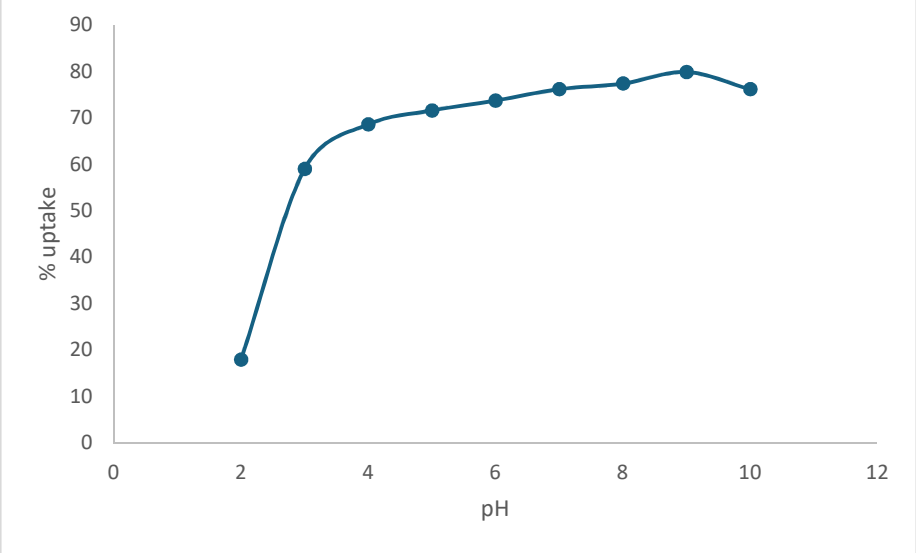

Figure 4.8: Effect of pH on the adsorption of CIP.

4.3 Adsorption Kinetics Studies

Adsorption kinetics studies are crucial for comprehending the underlying mechanisms controlling the pace at which an adsorbent, like BP, interacts with an

adsorbate, like CIP. To identify the regulating adsorption mechanism, experimental data is often fitted to multiple kinetic models, with the adsorption capacity being tracked over time.

4.3.1 Pseudo-First Order Kinetics Model

The pseudo-first order model, introduced by Lagergren (1898), is an adsorption kinetics model based on the assumption that the adsorption rate is directly proportional to the sites available. The following rate equation represents this model:

$$\log(q_e - q_t) = \log q_e - \frac{k_1}{2.303} t \qquad \textbf{[2]}$$

Where

q_e = Amount of adsorbate (CIP) adsorbed at equilibrium (mg/g)

q_t = Amount of adsorbate (CIP) adsorbed at time "t" (mg/g)

k_1 = Rate constant of the first order model (min^{-1})

t = Time (min)

For different CIP concentrations, a log (q_e – q_t) versus t graph was plotted. The PSO kinetic model for CIP sorption onto BP was shown in Figure 4.9. The values for q_e (calculated) and k_1 are obtained from the plot's y-intercept and slope, respectively. The R^2, q_e, and k_1 values were computed and compiled for every CIP concentration.

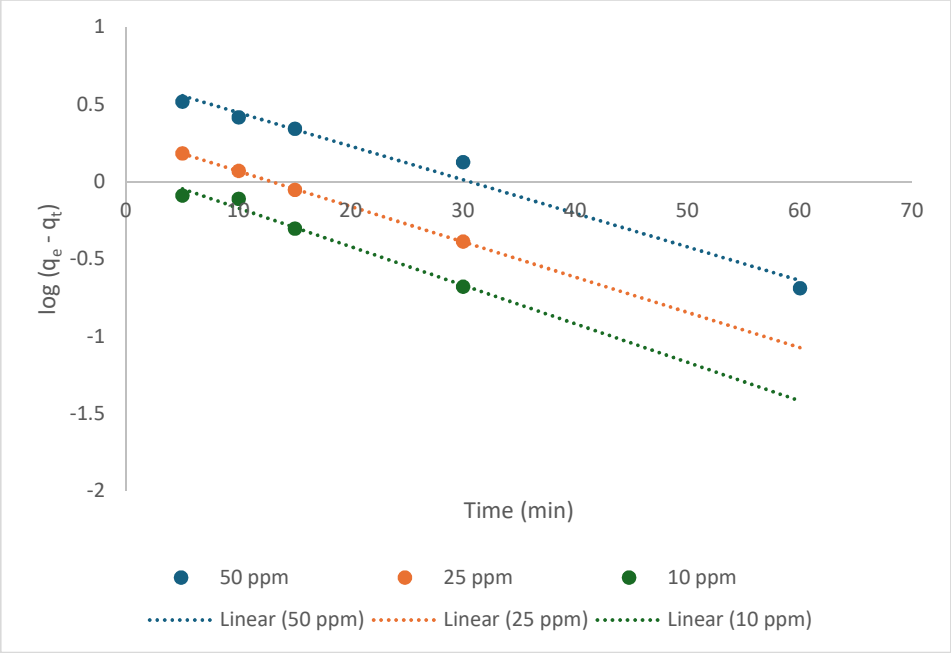

Figure 4.9: Pseudo-first order plot.

4.3.2 Pseudo-Second Order Kinetics Model

Ho and McKay (1999) created the pseudo-second-order model of adsorption kinetics, which postulates that chemisorption involving electron sharing or covalent bonding between the adsorbent and adsorbate regulates the adsorption rate. The following rate equation represents the model:

$$\frac{t}{q_t} = \frac{1}{h} + \frac{t}{q_e} \qquad [3]$$

Where

q_e = Amount of adsorbate (CIP) adsorbed at equilibrium (mg/g)

q_t = Amount of adsorbate (CIP) adsorbed at time "t" (mg/g)

k_1 = Rate constant of the first order model (min^{-1})

t = Time (min)

h = Initial adsorption rate (mg/g min)

The PSO kinetic model for the adsorption of CIP by BP is shown in Figure 4.10. The data points at 25 mg/L and 50 mg/L closely follow the linear trendlines, supporting that the pseudo-second-order model fits the adsorption at these concentrations. The strong linear correlation indicates that chemisorption, characterized by valence forces through electron sharing or exchange between the adsorbent and adsorbate, is likely responsible for controlling the adsorption process. The 10 mg/L data, on the other hand, exhibit a discernible departure from the linear fit, especially at longer contact durations. This variation indicates that, at lower initial concentrations, the adsorption process might deviate from pseudo-second-order kinetics.

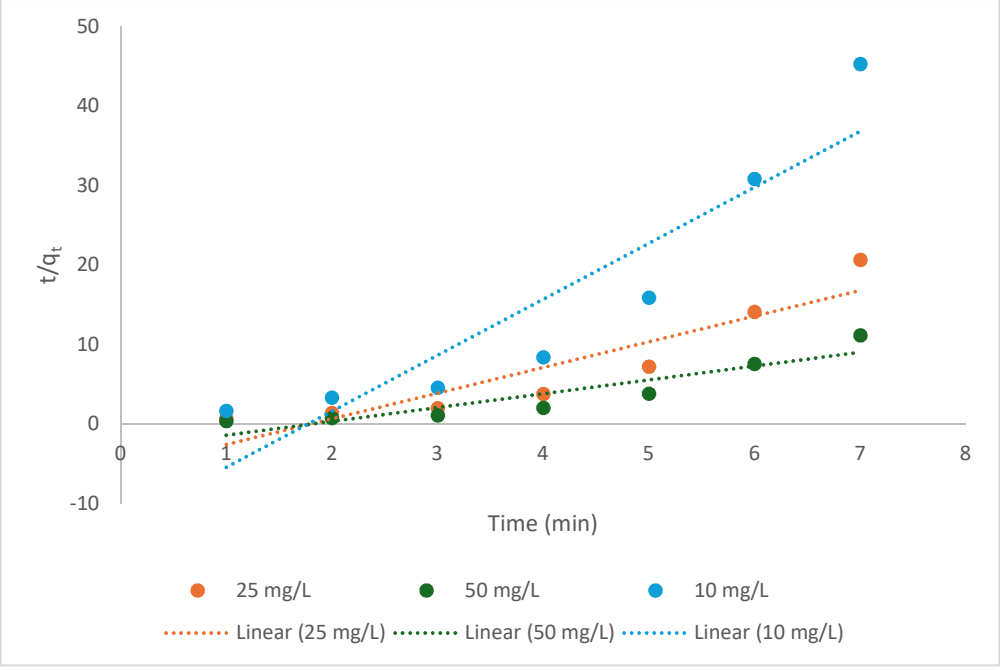

Figure 4.10: Pseudo-second order plot.

4.4 Adsorption Isotherm

The way a solute, usually a gas or liquid, sticks to a solid's surface at a steady temperature is depicted graphically by an adsorption isotherm. It describes the relationship between the concentration of a material in the surrounding phase at equilibrium and the quantity of material adsorbed per unit mass of the adsorbent.

Adsorption isotherm models vary, and they are all predicated on various surface and adsorption-related hypotheses. To identify the nature of CIP adsorption on the BP surface, the experimental data were fitted to the three models. The Langmuir isotherm suggests that after a molecule occupies a site on a uniform surface with a fixed number of sites, no more adsorptions can occur at that site, resulting in monolayer coverage. The Freundlich isotherm, on the other hand, is an empirical model that permits multilayer adsorption without a specific saturation point and takes into consideration adsorption on heterogeneous surfaces. Multilayer adsorption on solid surfaces is characterized by the BET (Brunauer–Emmett–Teller) isotherm, which builds upon the Langmuir isotherm by accounting for multiple adsorption layers. In contrast to the Langmuir model, which presumes monolayer coverage, the BET isotherm takes into consideration the potential for additional layers to form on top of the initial layer.

The models are applied to the experimental data to identify the isotherm that most accurately describes the CIP adsorption process onto BP. This allows for the identification of distinct adsorption patterns, including uniform monolayer adsorption, multilayer adsorption on a varied surface, and the creation of further layers after initial adsorption without additional interaction.

CHAPTER 5

CONCLUSION

5.1 Conclusion

In summary, this investigation effectively achieved its goals by proving BP to be a very effective adsorbent for CIP removal from aqueous solutions. The data revealed that BP exhibits considerable adsorption potential, following Pseudo-Second Order kinetics and fitting the Freundlich isotherm model effectively. Contact time, dye concentration, adsorbent dosage, pH, and agitation rate—all important factors influencing adsorption—were thoroughly examined. At lower CIP concentrations, BP exhibited a maximum adsorption of 37.037 mg/g, achieving a removal rate of 79.5%. By using Plackett-Burman, the influential factors found were contact time, pH and adsorbent dosage. Response surface methodology was used to determine the modified cubic model and the 3D surface plots of the relationships between the factors.

FTIR studies were conducted to determine the functional groups involved in the adsorption process. The observed changes in peak positions after adsorption provide evidence for the involvement of functional groups in the CIP-BP interaction. The technique' efficacy was also visually confirmed by SEM and AFM investigations, which showed notable changes in the BP's surface topography and morphology following adsorption.

These combined findings show that BP is a viable, environmentally friendly substitute for traditional adsorbents, providing a low-cost, sustainable way to

remove wastewater contaminated with antibiotics. The research offers a strong basis for additional research into BP modifications to increase their adsorption capability and expand their use in environmental cleanup.

5.2 Further Studies

The effectiveness of BP as an adsorbent is hindered by its limited adsorption capacity, weak mechanical properties, and poor long-term stability. Due to variations in peel composition, its performance is very pH dependent.

Chemical or physical alteration is a key strategy to enhance BPs as an adsorbent. BPs naturally contain functional groups such as hydroxyl, carboxyl, and amino groups, but the amount and accessibility of these groups are limited. To improve these qualities, BPs can be treated with bases (like NaOH) or acids (like HCl or H_2SO_4). While base treatment can reveal more hydroxyl groups that enhance heavy metal adsorption, acid treatment can increase the surface's positive charges, which improves its ability to adsorb negatively charged contaminants. Physical processes that enhance the surface area, including heating (carbonization) or grinding into finer granules, can also be considered to provide more surface area.

REFERENCES

ACS. 2016. *Ciprofloxacin, American Chemical Society* [Online]. Available at: https://www.acs.org/molecule-of-the-week/archive/c/ciprofloxacin.html [Accessed: 24 March 2025].

Adegoke, K.A. et al., 2023. Modified biomass adsorbents for removal of organic pollutants: A review of batch and Optimization Studies. *International Journal of Environmental Science and Technology*, 20(10), pp. 11615–11644. doi:10.1007/s13762-023-04872-2.

Agboola, O.S. and Bello, O.S., 2020. Enhanced adsorption of ciprofloxacin from aqueous solutions using functionalized banana stalk. *Biomass Conversion and Biorefinery*, 12(12), pp. 5463–5478. doi:10.1007/s13399-020-01038-9.

Ahmaruzzaman, Md., 2008. Adsorption of phenolic compounds on low-cost adsorbents: A Review. *Advances in Colloid and Interface Science*, 143(1–2), pp. 48–67. doi:10.1016/j.cis.2008.07.002.

Ajala, O.A. et al., 2023. Adsorptive removal of antibiotic pollutants from wastewater using biomass/biochar-based adsorbents. *RSC Advances*, 13(7), pp. 4678–4712. doi:10.1039/d2ra06436g.

Akhter, S. et al., 2024. Antibiotic residue contamination in the aquatic environment, sources and associated potential health risks. *Environmental Geochemistry and Health*, 46(10). doi:10.1007/s10653-024-02146-5.

Alawa, B. et al., 2025. Development of novel biochar adsorbent using agricultural waste biomass for enhanced removal of ciprofloxacin from water: Insights into the isotherm, kinetics, and thermodynamic analysis. *Chemosphere*, 375, p. 144252. doi:10.1016/j.chemosphere.2025.144252.

Al-Buriahi, A.K. et al., 2022. Ciprofloxacin removal from non-clinical environment: A critical review of current methods and future trend prospects. *Journal of Water Process Engineering*, 47, p. 102725. doi:10.1016/j.jwpe.2022.102725.

Andrade Siqueira, T.C. et al., 2020. Sugarcane bagasse as an efficient Biosorbent for methylene blue removal: Kinetics, isotherms and Thermodynamics. *International Journal of Environmental Research and Public Health*, 17(2), p. 526. doi:10.3390/ijerph17020526.

Arun, S. and Maharathi, P., 2019. Characterisation of biochar obtained from organic material and its application for removal of ciprofloxacin. *Oriental Journal of Chemistry*, 35(3), pp. 1086–1093. doi:10.13005/ojc/350323.

Arvia., 2024, *Ciprofloxacin wastewater treatment: Ciprofloxacin removal from water, Ciprofloxacin Wastewater Treatment | Ciprofloxacin Removal From Water* [Online]. Available at: https://arviatechnology.com/pollutants/ciprofloxacin-removal-from-water/ (Accessed: 24 March 2025).

Azzam, A.B. et al., 2023. Heterogeneous porous biochar-supported nano NIFE2O4 for efficient removal of hazardous antibiotic from pharmaceutical wastewater. *Environmental Science and Pollution Research*, 30(56), pp. 119473–119490. doi:10.1007/s11356-023-30587-5.

Balarak, D. et al., 2021. Adsorption of ciprofloxacin from aqueous solution onto synthesized nio: Isotherm, kinetic and thermodynamic studies. *Desalination and Water Treatment*, 212, pp. 390–400. doi:10.5004/dwt.2021.26603.

Balarak, D., Zafariyan, M. and Siddiqui, S., 2022. Investigation of adsorptive properties of surfactant modified sepiolite for removal of ciprofloxacin. *International Journal of Life Science and Pharma Research* [Preprint]. doi:10.22376/ijpbs/lpr.2020.10.3.p12-19.

Balouch, A. et al., 2013. Sorption kinetics, isotherm and thermodynamic modeling of defluoridation of ground water using natural adsorbents. *American Journal of Analytical Chemistry*, 04(05), pp. 221–228. doi:10.4236/ajac.2013.45028.

Bansal, R.C. and Goyal, M., 2005. *Activated carbon adsorption*. Boca Raton, Florida: Taylor & Francis.

Boehm, H.P., 1994. Some aspects of the surface chemistry of carbon blacks and other carbons. *Carbon*, 32(5), pp. 759–769. doi:10.1016/0008-6223(94)90031-0.

Brunauer, S., Emmett, P.H. and Teller, E., 1938. Adsorption of gases in multimolecular layers. *Journal of the American Chemical Society*, 60(2), pp. 309–319. doi:10.1021/ja01269a023.

Bui, Q.M. et al., 2023. Removal of fluoroquinolone antibiotics by chitosan–magnetite from aqueous: Single and binary adsorption. *Processes*, 11(8), p. 2396. doi:10.3390/pr11082396.

Campos, V.N. et al., 2024. High performance of ciprofloxacin removal using heterostructure material based on the combination of CeO_2 and palygorskite fibrous clay. *Minerals*, 14(8), p. 792. doi:10.3390/min14080792.

Conley, Z.C. et al., 2018. Wicked: The untold story of ciprofloxacin. *PLOS Pathogens*, 14(3). doi:10.1371/journal.ppat.1006805.

Darvishi, P. et al., 2023. A comprehensive review on the removal of antibiotics from water and wastewater using carbon nanotubes: Synthesis, performance, and future challenges. *Environmental Science: Water Research; Technology*, 9(1), pp. 11–37. doi:10.1039/d1ew00912e.

Das, S. and Sengupta, S., 2023). Sustainable removal of antibiotic drugs from wastewater using different adsorbents—A concise review. *Water Conservation Science and Engineering*, 8(1). doi:10.1007/s41101-023-00180-5.

Daughton, C.G. and Ternes, T.A., 1999. Pharmaceuticals and personal care products in the environment: Agents of subtle change?. *Environmental Health Perspectives*, 107(suppl 6), pp. 907–938. doi:10.1289/ehp.99107s6907.

Dias, J.M. et al., 2007. Waste materials for activated carbon preparation and its use in aqueous-phase treatment: A Review. *Journal of Environmental Management*, 85(4), pp. 833–846. doi:10.1016/j.jenvman.2007.07.031.

Eniola, J.O., Kumar, R. and Barakat, M.A., 2019. Adsorptive removal of antibiotics from water over natural and modified adsorbents. *Environmental Science and Pollution Research*, 26(34), pp. 34775–34788. doi:10.1007/s11356-019-06641-6.

Ertaş, M. et al., 2010. Removal of methylene blue from aqueous solution using cotton stalk, cotton waste and cotton dust. *Journal of Hazardous Materials*, 183(1–3), pp. 421–427. doi:10.1016/j.jhazmat.2010.07.041.

Filote, C. et al., 2021. Sustainable application of Biosorption and bioaccumulation of persistent pollutants in wastewater treatment: Current practice. *Processes*, 9(10), p. 1696. doi:10.3390/pr9101696.

Foo, K.Y. and Hameed, B.H., 2010. Insights into the modeling of adsorption isotherm systems. *Chemical Engineering Journal*, 156(1), pp. 2–10. doi:10.1016/j.cej.2009.09.013.

Gargiulo, V., Di Natale, F. and Alfe, M., 2024. From agricultural wastes to advanced materials for environmental applications: Rice husk-derived adsorbents for heavy metals removal from wastewater. *Journal of Environmental Chemical Engineering*, 12(5), p. 113497. doi:10.1016/j.jece.2024.113497.

Grada, A. and Bunick, C.G., 2021. Spectrum of antibiotic activity and its relevance to the microbiome. *JAMA Network Open*, 4(4). doi:10.1001/jamanetworkopen.2021.5357.

Gregg, S.J. and Sing, K.S.W., 1997. *Adsorption, surface area and porosity*. London, UK: Academic Press.

Gupta, S.S., Al Kausor, M. and Chakrabortty, D., 2025. Banana peel as potential bioadsorbent toward removal of emerging contaminants from wastewater for sustainable environment: A Review. *Chemical Papers* [Preprint]. doi:10.1007/s11696-025-03945-5.

Gupta, V.K. et al., 2012. Chemical Treatment Technologies for waste-water recycling—an overview. *RSC Advances*, 2(16), p. 6380. doi:10.1039/c2ra20340e.

Gupta, V.K., Nayak, A. and Agarwal, S., 2015. Bioadsorbents for remediation of heavy metals: Current status and their future prospects. *Environmental Engineering Research*, 20(1), pp. 1–18. doi:10.4491/eer.2015.018.

Hettithanthri, O. et al., 2022. Colloidal biochar for enhanced adsorption of antibiotic ciprofloxacin in aqueous and synthetic hydrolyzed human urine matrices. *Chemosphere*, 297, p. 133984. doi:10.1016/j.chemosphere.2022.133984.

Ho, Y.S. and McKay, G., 1999. Pseudo-second order model for Sorption Processes. *Process Biochemistry*, 34(5), pp. 451–465. doi:10.1016/s0032-9592(98)00112-5.

Ioannidou, O. and Zabaniotou, A., 2007. Agricultural residues as precursors for activated carbon production—a review. *Renewable and Sustainable Energy Reviews*, 11(9), pp. 1966–2005. doi:10.1016/j.rser.2006.03.013.

Jahin, H.S., Khedr, A.I. and Ghannam, H.E., 2024. Banana peels as a green bioadsorbent for removing metals ions from wastewater. *Discover Water*, 4(1), p.36. doi:10.1007/s43832-024-00080-2.

Käärik, M. et al., 2024. Nanomaterial texture-based machine learning of ciprofloxacin adsorption on nanoporous carbon. *International Journal of Molecular Sciences*, 25(21), p. 11696. doi:10.3390/ijms252111696.

Karim, A.M. et al., 2024. Linear and Nonlinear Approach on Kinetic Studies in the Adsorption of Ciprofloxacin onto Banana Peels-base Carbon from Aqueous Solution. *Journal of Science and Engineering Papers*, 01(02), pp. 73–80. doi:10.62275/josep.24.1000001.

Khamsucharit, P. et al., 2017. Characterization of pectin extracted from banana peels of different varieties. *Food Science and Biotechnology*, 27(3), pp. 623–629. doi:10.1007/s10068-017-0302-0.

Kümmerer, K., 2008, *Pharmaceuticals in the environment: Sources, fate, effects, and risks*. Berlin, Heidelberg: Springer.

Kümmerer, K., 2009. Antibiotics in the aquatic environment – a review – part I. *Chemosphere*, 75(4), pp. 417–434. doi:10.1016/j.chemosphere.2008.11.086.

Langmuir, I., 1918. The adsorption of gases on plane surfaces of glass, mica and platinum. *Journal of the American Chemical Society*, 40(9), pp. 1361–1403. doi:10.1021/ja02242a004.

Li, R. et al., 2018. Adsorptive removal of antibiotics from water using peanut shells from agricultural waste. *RSC Advances*, 8(24), pp. 13546–13555. doi:10.1039/c7ra11796e.

Li, Y.-H. et al., 2003. Adsorption of cadmium(ii) from aqueous solution by surface oxidized carbon nanotubes. *Carbon*, 41(5), pp. 1057–1062. doi:10.1016/s0008-6223(02)00440-2.

Liu, P. et al., 2023. The efficient removal of Congo red and ciprofloxacin by peony seeds shell activated carbon with ultra-high specific surface area. *Environmental Science and Pollution Research*, 30(18), pp. 53177–53190. doi:10.1007/s11356-023-26146-7.

Lowell, S. et al., 2004. Characterization of porous solids and powders: Surface area, pore size and density. *Particle Technology Series* [Preprint]. doi:10.1007/978-1-4020-2303-3.

Lu, D. et al., 2020. Adsorption and desorption behaviors of antibiotic ciprofloxacin on functionalized spherical MCM-41 for water treatment. *Journal of Cleaner Production*, 264, p. 121644. doi:10.1016/j.jclepro.2020.121644.

Meseguer, V.F. et al., 2024. Ciprofloxacin uptake from an aqueous solution via adsorption with K2CO3-activated biochar derived from brewing industry bagasse. *Processes*, 12(1), p. 199. doi:10.3390/pr12010199.

Moreno-Castilla, C., 2004. Adsorption of organic molecules from aqueous solutions on Carbon Materials. *Carbon*, 42(1), pp. 83–94. doi:10.1016/j.carbon.2003.09.022.

Mu, X. et al., 2023. Impact of antibiotics on microbial community in aquatic environment and Biodegradation Mechanism: A review and Bibliometric Analysis. *Environmental Science and Pollution Research*, 30(25), pp. 66431–66444. doi:10.1007/s11356-023-27018-w.

Magesh, N. et al., 2021. Adsorption of ciprofloxacin from aqueous solution using surface improved tamarind shell as an economical and effective adsorbent. *International Journal of Phytoremediation*, 24(3), pp. 224–234. doi:10.1080/15226514.2021.1932730.

Naganathan, K.K. et al., 2021. Adsorptive removal of bisphenol A from aqueous solution using activated carbon from coffee residue. *Materials Today: Proceedings*, 47, pp. 1307–1312. doi:10.1016/j.matpr.2021.02.802.

Nyong, B.E. et al., 2024. Lignocellulosic and Bioactive Composition of Banana Peels for Pharmacological Applications. *International Journal of Health and Pharmaceutical Research*, 9(4), pp. 92–103. doi:10.56201/ijhpr.v9.no4.2024.pg92.103.

OECD., 2022. Limiting Environmental Impacts of Unused or Expired Medicine. *Management of Pharmaceutical Household Waste* [Preprint]. doi:10.1787/3854026c-en.

Pabst, S., 2023, *Antimicrobial resistance, World Health Organization* [Online]. Available at: https://www.who.int/news-room/fact-sheets/detail/antimicrobial-resistance (Accessed: 11 February 2025).

Patel, M. et al., 2021. Ciprofloxacin and acetaminophen sorption onto Banana Peel biochars: Environmental and process parameter influences. *Environmental Research*, 201, p. 111218. doi:10.1016/j.envres.2021.111218.

Pham, T.D. et al., 2023. Adsorption characteristics of ciprofloxacin and naproxen from aqueous solution using bamboo biochar. *Biomass Conversion and Biorefinery*, 15(2), pp. 3071–3082. doi:10.1007/s13399-023-05092-x.

Plackett, R.L. and Burman, J.P., 1946 The design of optimum multifactorial experiments. *Biometrika*, 33(4), pp. 305–325. doi:10.1093/biomet/33.4.305.

Salah, H. et al., 2024. Management of a ciprofloxacin as a contaminant of emerging concern in water using microalgaebioremediation: Mechanism, modeling, and Kinetic Studies. *Microbial Cell Factories*, 23(1). doi:10.1186/s12934-024-02591-y.

Sangeetha Piriya, R. et al., 2021. Coconut shell derived ZNCL2 activated carbon for malachite green dye removal. *Water Science and Technology*, 83(5), pp. 1167–1182. doi:10.2166/wst.2021.050.

Sanni, S.O. et al., 2024. Removal of tetracycline from the aquatic environment using activated carbon: A comparative study of adsorption performance based on the activator agents. *Heliyon*, 10(14). doi:10.1016/j.heliyon.2024.e34637.

Shan, R. et al., 2020. Single and competitive adsorption affinity of heavy metals toward peanut shell-derived biochar and its mechanisms in aqueous systems. *Chinese Journal of Chemical Engineering*, 28(5), pp. 1375–1383. doi:10.1016/j.cjche.2020.02.012.

Su, D. et al., 2024. Removing efficiency and mechanism of ciprofloxacin from aqueous solution using rectorite. *Water, Air, & Soil Pollution*, 235(5). doi:10.1007/s11270-024-07070-z.

Upmanyu, N. and Malviya, V.N., 2020. Antibiotics: Mechanisms of action and modern challenges. *Microorganisms for Sustainable Environment and Health*, pp. 367–382. doi:10.1016/b978-0-12-819001-2.00018-8.

Volesky, B. and Holan, Z.R., 1995. Biosorption of heavy metals. *Biotechnology Progress*, 11(3), pp. 235–250. doi:10.1021/bp00033a001.

Wang, S. and Zhu, Z., 2007. Effects of acidic treatment of activated carbons on dye adsorption. *Dyes and Pigments*, 75(2), pp. 306–314. doi:10.1016/j.dyepig.2006.06.005.

Weber, W.J. and Morris, J.C., 1963. Kinetics of adsorption on carbon from solution. *Journal of the Sanitary Engineering Division*, 89(2), pp. 31–59. doi:10.1061/jsedai.0000430.

World Health Organization., 2012. *Pharmaceuticals in drinking-water*. Geneva, Switzerland: World Health Organization.

Yadav, M.S. et al., 2022. Competitive adsorption analysis of antibiotics removal from multi-component systems using chemically activated spent tea waste: Effect of operational parameters, kinetics, and Equilibrium Study. *Environmental Science and Pollution Research*, 30(15), pp. 42697–42712. doi:10.1007/s11356-022-22323-2.

Yu, X., Zipp, G.L. and Davidson III, G.W., 1994. The Effect of Temperature and pH on the Solubility of Quinolone Compounds: Estimation of Heat of Fusion. *Pharmaceutical Research*, 11(4), pp. 522–527. doi:10.1023/a:1018910431216.

APPENDICES

Appendix A: Standard Calibration Curve

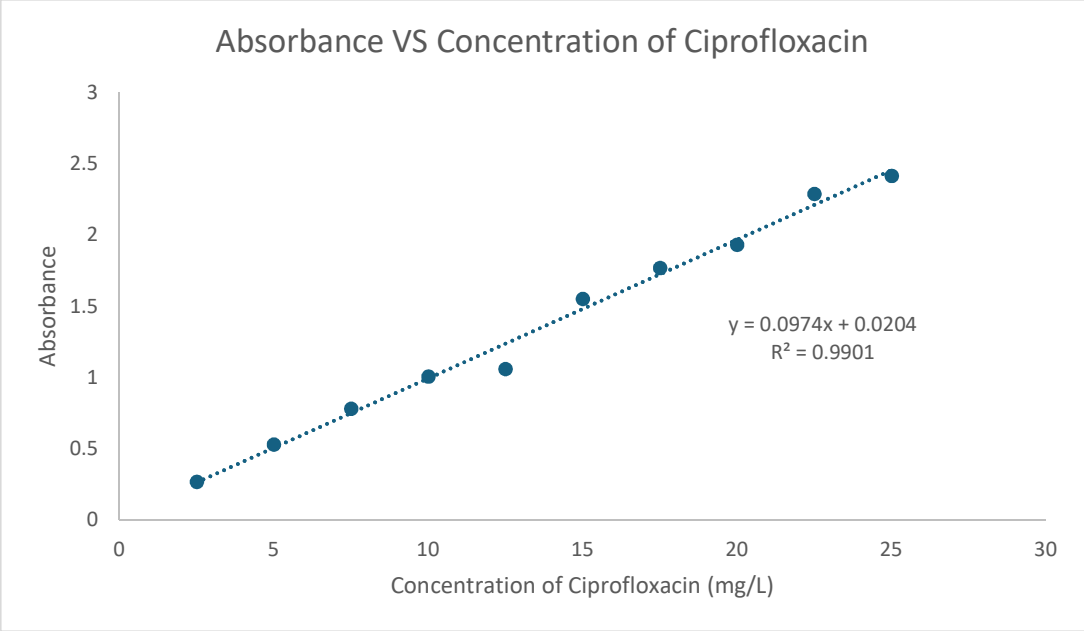

Equation: $y = 0.0974x + 0.0204$